Eur. Phys. J. C (2018) 78:589
https://doi.org/10.1140/epjc/s10052-018-6049-9

THE EUROPEAN PHYSICAL JOURNAL C

CrossMark

Regular Article - Experimental Physics

Electroweak production of two jets in association with a Z boson in proton–proton collisions at $\sqrt{s} = 13\,\text{TeV}$

CMS Collaboration*

CERN, 1211 Geneva 23, Switzerland

Received: 28 December 2017 / Accepted: 4 July 2018
© CERN for the benefit of the CMS collaboration 2018

Abstract A measurement of the electroweak (EW) production of two jets in association with a Z boson in proton-proton collisions at $\sqrt{s} = 13\,\text{TeV}$ is presented, based on data recorded in 2016 by the CMS experiment at the LHC corresponding to an integrated luminosity of $35.9\,\text{fb}^{-1}$. The measurement is performed in the $\ell\ell$jj final state with ℓ including electrons and muons, and the jets j corresponding to the quarks produced in the hard interaction. The measured cross section in a kinematic region defined by invariant masses $m_{\ell\ell} > 50\,\text{GeV}$, $m_{\text{jj}} > 120\,\text{GeV}$, and transverse momenta $p_{\text{Tj}} > 25\,\text{GeV}$ is $\sigma_{\text{EW}}(\ell\ell\text{jj}) = 534 \pm 20\,(\text{stat}) \pm 57\,(\text{syst})\,\text{fb}$, in agreement with leading-order standard model predictions. The final state is also used to perform a search for anomalous trilinear gauge couplings. No evidence is found and limits on anomalous trilinear gauge couplings associated with dimension-six operators are given in the framework of an effective field theory. The corresponding 95% confidence level intervals are $-2.6 < c_{WWW}/\Lambda^2 < 2.6\,\text{TeV}^{-2}$ and $-8.4 < c_W/\Lambda^2 < 10.1\,\text{TeV}^{-2}$. The additional jet activity of events in a signal-enriched region is also studied, and the measurements are in agreement with predictions.

1 Introduction

In proton-proton (pp) collisions at the CERN LHC, the production of dileptons ($\ell\ell$) consistent with the Z boson invariant mass in association with two jets (jj) is dominated by events where the dilepton pair is produced by a Drell–Yan (DY) process, in association with jets from strong interactions. This production is governed by a mixture of electroweak (EW) and strong processes of order $\alpha_{\text{EW}}^2\alpha_{\text{S}}^2$, where α_{S} is the strong coupling and α_{EW} is the EW coupling strength.

The pure electroweak production of the $\ell\ell$jj final state, at order α_{EW}^4, is less frequent [1], and includes production via the vector boson fusion (VBF) process, with its distinctive signature of two jets with both large energy and separation in pseudorapidity η. In this paper the electroweak production is referred to as EW Zjj, and the two jets produced through the fragmentation of the outgoing quarks are referred to as "tagging jets".

Figure 1 shows representative Feynman diagrams for the EW Zjj signal, namely VBF (left), bremsstrahlung-like (center), and multiperipheral (right) production. Gauge cancellations lead to a large negative interference between the VBF process and the other two processes, with the interferences from the bremsstrahlung-like production being larger. Interference with multiperipheral production is limited to cases where the dilepton mass is close to the Z boson peak mass [2].

In the inclusive production of $\ell\ell$jj final states, some of the nonexclusive EW interactions with identical initial and final states can interfere with the exclusive EW interactions that are shown in Fig. 1. This interference effect between the signal production and the main background processes is much smaller than the interference effects among the EW production amplitudes, but needs to be taken into account when measuring the signal contribution [3,4].

Figure 2 (left) shows one example of corrections to order α_{S}^2 for DY production that have the same initial and final states as those in Fig. 1. A process at order α_{S}^2 that does not interfere with the EW signal is shown in Fig. 2 (right).

The study of EW Zjj processes is part of a more general investigation of standard model (SM) vector boson fusion and scattering processes that include studies of Higgs boson production [5–7] and searches for physics beyond the SM [8–11]. When isolated from the backgrounds, the properties of EW Zjj events can be compared with SM predictions. Probing the additional hadronic activity in selected events can shed light on the modelling of additional parton radiation [12,13], which is important for signal selection or vetoing of background events.

New physics could appear in the form of anomalous trilinear gauge couplings (ATGCs) [14,15] that can be parameterized with higher-dimensional operators. Their measure-

* e-mail: cms-publication-committee-chair@cern.ch

Published online: 20 July 2018

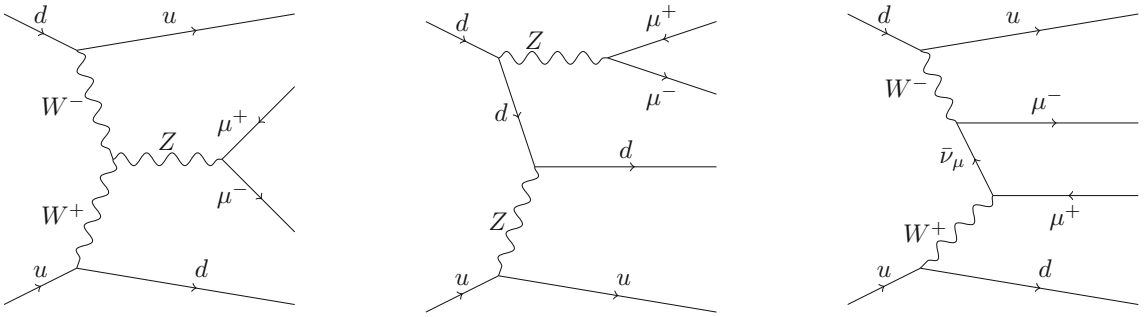


Fig. 1 Representative Feynman diagrams for purely electroweak amplitudes for dilepton production in association with two jets: vector boson fusion (left), bremsstrahlung-like (center), and multiperipheral production (right)

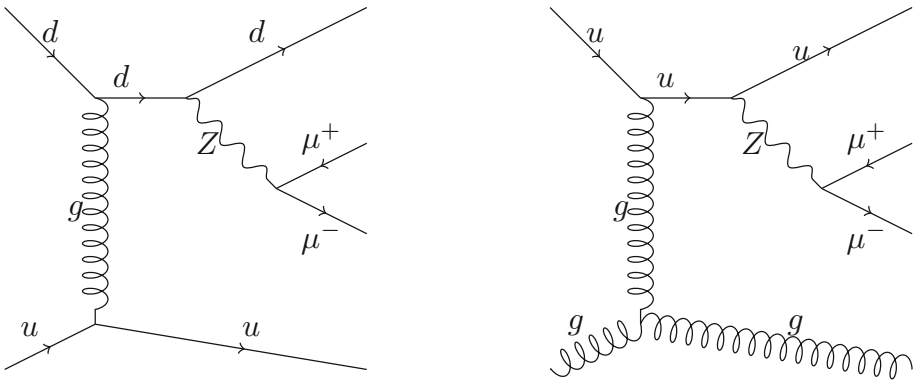


Fig. 2 Representative Feynman diagrams for order α_S^2 corrections to DY production that constitute the main background for the measurement

ments could provide an indirect search for new physics at mass scales not directly accessible at the LHC.

At the LHC, the EW Zjj process was first measured by the CMS experiment using pp collisions at $\sqrt{s} = 7$ TeV [3], and then at $\sqrt{s} = 8$ TeV by both the CMS [4] and ATLAS [16] experiments. The ATLAS experiment has also performed measurements at $\sqrt{s} = 13$ TeV [17], with a data sample corresponding to an integrated luminosity of $3.2\,\text{fb}^{-1}$. All results so far agree with the expectations of the SM within a precision of approximately 20%.

This paper presents a measurement with the CMS detector using pp collisions collected at $\sqrt{s} = 13$ TeV during 2016, corresponding to an integrated luminosity of $35.9\,\text{fb}^{-1}$. A multivariate analysis, based on the methods developed for the 7 and 8 TeV data results [3,4], is used to separate signal events from the large DY + jets background. Analysis of the 13 TeV data with larger integrated luminosity and larger predicted total cross section offers an opportunity to measure the cross section at a higher energy and reduce the uncertainties of the earlier measurements.

Section 2 describes the experimental apparatus and Sect. 3 the event simulations. Event selection procedures are described in Sect. 4, together with the selection efficiencies and background models in control regions. Section 5 details the strategy adopted to extract the signal from the data, and the corresponding systematic uncertainties are summarized in Sect. 6. The cross section and anomalous coupling results are presented in Sects. 7 and 8, respectively. Section 9 provides a study of the additional hadronic activity in an EW Zjj-enriched region. Finally, a brief summary of the results is given in Sect. 10.

2 The CMS detector

The central feature of the CMS apparatus is a superconducting solenoid of 6 m internal diameter, providing a magnetic field of 3.8 T. Within the solenoid volume are a silicon pixel and strip tracker, a lead tungstate crystal electromagnetic calorimeter (ECAL), and a brass and scintillator hadron calorimeter (HCAL), each composed of a barrel and two endcap sections. Forward calorimeters extend the η coverage provided by the barrel and endcap detectors. Muons are measured in gas-ionization detectors embedded in the steel flux-return yoke outside the solenoid.

The tracker measures charged particles within the pseudorapidity range $|\eta| < 2.5$. It consists of 1440 pixel and 15 148 strip detector modules. For nonisolated particles of $1 < p_T < 10$ GeV and $|\eta| < 1.4$, the track resolutions are typically 1.5% in p_T and 25–90 (45–150) μm in the transverse (longitudinal) impact parameter [18].

The electron momenta are estimated by combining energy measurements in the ECAL with momentum measurements in the tracker [19]. The dielectron invariant mass resolution

for Z $\rightarrow$ ee decays is 1.9% when both electrons are in the ECAL barrel, and 2.9% when both electrons are in the endcaps.

Muons are measured in the pseudorapidity range $|\eta| < 2.4$ with detection planes made using three technologies: drift tubes, cathode strip chambers, and resistive-plate chambers. Matching muons to tracks measured in the silicon tracker results in a relative transverse momentum resolution for muons with $20 < p_{\mathrm{T}} < 100$ GeV of 1.3–2.0% in the barrel and better than 6% in the endcaps. The p_{T} resolution in the barrel is better than 10% for muons with p_{T} up to 1 TeV [20].

The offline analysis uses reconstructed charged-particle tracks and candidates from the particle-flow (PF) algorithm [21]. In the PF event reconstruction, all stable particles in the event, i.e. electrons, muons, photons, charged and neutral hadrons, are reconstructed as PF candidates using information from all subdetectors to obtain an optimal determination of their direction, energy, and type. The PF candidates are then used to reconstruct the jets and the missing transverse momentum.

A more detailed description of the CMS detector, together with a definition of the coordinate system and the relevant kinematic variables, can be found in Ref. [22].

3 Simulation of signal and background events

Signal events are simulated at leading order (LO) using the MadGraph5_aMC@NLO (v2.3.3) Monte Carlo (MC) generator [23,24], interfaced with pythia (v8.212) [25,26] for parton showering (PS) and hadronization. The NNPDF30 (nlo_as0130) [27] parton distribution functions (PDF) are used to generate the events. The underlying event (UE) is modelled using the CUETP8M1 tune [28]. The simulation does not include extra partons at matrix element (ME) level. The signal is defined in the kinematic region with dilepton invariant mass $m_{\ell\ell} > 50$ GeV, parton transverse momentum $p_{\mathrm{Tj}} > 25$ GeV, and diparton invariant mass $m_{\mathrm{jj}} > 120$ GeV. The cross section of the $\ell\ell$jj final state (with ℓ = e or μ), applying the above fiducial cuts, is calculated to be $\sigma_{\mathrm{LO}}(\mathrm{EW}\ \ell\ell\mathrm{jj}) = 543^{+7}_{-9}\,(\mathrm{scale}) \pm 22\,(\mathrm{PDF})$ fb, where the first uncertainty is obtained by changing simultaneously the factorization (μ_{F}) and renormalization (μ_{R}) scales by factors of 2 and 1/2, and the second reflects the uncertainties in the NNPDF30 PDFs. The LO signal cross section and relevant kinematic distributions estimated with MadGraph5_aMC@NLO are found to be in agreement within 5% with the next-to-leading order (NLO) predictions of the VBFNLO generator (v.2.7.1) [29–31] that includes NLO QCD corrections. For additional comparisons, signal events have also been simulated with the Herwig++ (v2.7.1) [32] PS, using the EE5C [33] tune.

Events coming from processes including ATGCs are generated with the same setting as the SM sample, but include additional information for reweighting in a three-dimensional effective field theory (EFT) parameter space, as described in more detail in Sect. 8.1.

Background DY events are also simulated with MadGraph5_aMC@NLO using (1) an NLO ME calculation with up to three final-state partons generated from quantum chromodynamics (QCD) interactions, and (2) an LO ME calculation with up to four partons. The ME-PS matching is performed following the FxFx prescription [34] for the NLO case, and the MLM prescription [35,36] for the LO case. The NLO background simulation is used to extract the final results, while the independent LO samples are used to perform the multivariate discriminant training. The dilepton DY production for $m_{\ell\ell} > 50$ GeV is normalized to $\sigma_{\mathrm{th}}(\mathrm{DY}) = 5.765$ nb, which is computed at next-to-next-to-leading order (NNLO) with fewz (v3.1) [37].

The evaluation of the interference between EW Zjj and DY Zjj processes relies on predictions obtained with MadGraph5_aMC@NLO. A dedicated sample of events arising from the interference terms is generated directly by selecting the contributions of order $\alpha_{\mathrm{S}}\alpha^{3}_{\mathrm{EW}}$, and passing them through the full detector simulation to estimate the expected interference contribution.

Other backgrounds are expected from other sources of events with two opposite-sign and same-flavour leptons together with jets. Top quark pair events are generated with powheg (v2.0) [38–40] and normalized to the inclusive cross section calculated at NNLO together with next-to-next-to-leading logarithmic corrections [41,42]. Single top quark processes are modelled at NLO with powheg [38–40,43,44] and normalized to cross sections of 71.7 ± 2.0 pb, 217 ± 3 pb, and 10.32 ± 0.20 pb respectively for the tW, t-, and s-channel production [41,45]. The diboson production processes WW, WZ, and ZZ are generated with pythia and normalized to NNLO cross section computations obtained with mcfm (v8.0) [46]. The abbreviation VV is used in this document when referring to the sum of the processes that yield two vector bosons.

The contribution from diboson processes with $\ell\ell$jj final states, such as ZW and ZZ, to the signal definition is small, and these contributions are not included in the background.

The production of a W boson in association with jets, where the W decays to a charged lepton and a neutrino, is also simulated with MadGraph5_aMC@NLO, and normalized to a total cross section of 61.53 nb, computed at NNLO with fewz. Multijet QCD processes are also studied in simulation, but are found to yield negligible contributions to the selected events. All background productions make use of the pythia PS model with the CUETP8M1 tune.

A detector simulation based on Geant4 (v.9.4p03) [47,48] is applied to all the generated signal and background sam-

ples. The presence of multiple pp interactions in the same bunch crossing (pileup) is incorporated by simulating additional interactions (both in-time and out-of-time with respect to the hard interaction) with a multiplicity that matches the distribution observed in data. The additional events are simulated with PYTHIA (v8.212) making use of the NNPDF23 (nlo_as0130) [49] PDF, and the CUETP8M1 tune. The average pileup is estimated to be about 27 additional interactions per bunch crossing.

4 Reconstruction and selection of events

Events containing two isolated, high-p_{T} leptons, and at least two high-p_{T} jets are selected. Isolated single-lepton triggers are used to acquire the data, where the lepton is required to have $p_{\mathrm{T}} > 27\,\mathrm{GeV}$ for the electron trigger and $p_{\mathrm{T}} > 24\,\mathrm{GeV}$ for the muon trigger [50].

In the offline reconstruction, electrons are reconstructed from clusters of energy deposits in the ECAL that match tracks extrapolated from the silicon tracker [19]. Offline muons are reconstructed by fitting trajectories based on hits in the silicon tracker and in the muon system [20]. Reconstructed electron or muon candidates are required to have $p_{\mathrm{T}} > 20\,\mathrm{GeV}$. Electron candidates are required to be reconstructed within $|\eta| \leq 2.4$, excluding barrel-to-endcap $1.444 < |\eta| < 1.566$ transition regions of the ECAL [22]. Muon candidates are required to be reconstructed in the fiducial region $|\eta| \leq 2.4$ of the muon system. The track associated with a lepton candidate is required to have both its transverse and longitudinal impact parameters compatible with the position of the main primary vertex (PV) of the event. The reconstructed PV with the largest value of summed physics-object p_{T}^2 is taken to be the primary pp interaction vertex. The physics objects are the objects returned by a jet finding algorithm [51,52] applied to all charged particle tracks associated with the vertex, plus the corresponding associated missing transverse momentum.

The leptons are required to be isolated. The isolation is calculated from particle candidates reconstructed by the PF algorithm and is corrected for pileup on an event-by-event basis. The sum of scalar p_{T} of all particle candidates reconstructed in an isolation cone with radius $R = \sqrt{(\Delta\eta)^2 + (\Delta\phi)^2} = 0.4$ around the momentum vector of the lepton is required to be below 15 (25)% of the electron (muon) p_{T} value. The two isolated leptons with opposite electric charge and highest p_{T} are chosen to form the dilepton pair, and are required to have $p_{\mathrm{T}} > 30\,\mathrm{GeV}$ and $p_{\mathrm{T}} > 20\,\mathrm{GeV}$ for the p_{T}-leading and subleading lepton, respectively. Events with additional leptons are kept in the event selection. Same-flavour dileptons (ee or $\mu\mu$) compatible with $\mathrm{Z} \to \ell\ell$ decays are then selected by requiring $|m_{\mathrm{Z}} - m_{\ell\ell}| < 15\,\mathrm{GeV}$, where m_{Z} is the mass of the Z boson [53].

Jets are reconstructed by clustering PF candidates with the anti-k_{T} algorithm [51,54] using a distance parameter of 0.4. The jet momentum is determined as the vector sum of all particle momenta in the jet, and is found from simulation to be within 5 to 10% of the true momentum over the whole p_{T} spectrum and detector acceptance [21].

An offset correction is applied to jet energies to take into account the contribution from additional proton-proton interactions within the same or nearby bunch crossings. Jet energy corrections are derived from simulation, and are confirmed with in situ measurements of the energy balance in dijet, multijet, photon + jet, and leptonically decaying Z + jet events [55]. Loose jet identification criteria are applied to reject misconstructed jets resulting from detector noise [56]. Loose criteria are also applied to remove jets heavily contaminated with pileup energy (clustering of energy deposits not associated with a parton from the primary pp interaction) [56,57]. The efficiency of the jet identification criteria is greater than 99%, rejecting 90% of background pileup jets with $p_{\mathrm{T}} \simeq 50\,\mathrm{GeV}$. The jet energy resolution (JER) is typically $\approx$15% at 10 GeV, 8% at 100 GeV, and 4% at 1 TeV [55]. Jets reconstructed with $p_{\mathrm{T}} \geq 15\,\mathrm{GeV}$ and $|\eta| \leq 4.7$ are used in the analysis.

The two highest p_{T} jets are defined as the tagging jets, and are required to have $p_{\mathrm{T}} > 50\,\mathrm{GeV}$ and $p_{\mathrm{T}} > 30\,\mathrm{GeV}$ for the p_{T}-leading and subleading jet, respectively. The invariant mass of the two tagging jets is required to satisfy $m_{\mathrm{jj}} > 200\,\mathrm{GeV}$.

A multivariate analysis technique, described in Sect. 5, is used to provide an optimal separation of the DY Zjj and EW Zjj components of the inclusive $\ell\ell$jj spectrum. The main discriminating variables are the dijet invariant mass m_{jj} and the pseudorapidity separation $\Delta\eta_{\mathrm{jj}}$. Other variables used in the multivariate analysis are described below.

Table 1 reports the expected and observed event yields after the initial selection and after imposing a minimum value for the final discriminator output that defines the signal-enriched region used for the studies of additional hadronic activity described in Sect. 9.

4.1 Discriminating gluons from quarks

Jets in signal events are expected to originate from quarks, while for background events it is more probable that jets are initiated by a gluon. A quark-gluon likelihood (QGL) discriminant [3] is evaluated for the two tagging jets with the intent of distinguishing the nature of each jet.

The QGL discriminant exploits differences in the showering and fragmentation of gluons and quarks by making use of the following internal jet composition observables: (1) the particle multiplicity of the jet, (2) the minor root-mean-square of distance between the jet constituents in the

Table 1 Event yields expected for background and signal processes using the initial selections and with a cut on the multivariate analysis output (BDT) that provides signal ≈ background. The yields are compared to the data observed in the different channels and categories. The total uncertainties quoted for signal, DY Zjj, dibosons, and processes with top quarks ($t\bar{t}$ and single top quarks) include the simulation statistical uncertainty

Sample	Initial		BDT > 0.92	
	ee	$\mu\mu$	ee	$\mu\mu$
WW	62 ± 16	116 ± 22	–	–
WZ	914 ± 38	2151 ± 63	1.6 ± 1.6	1.8 ± 1.8
ZZ	522 ± 17	1324 ± 29	1.8 ± 1.1	2.7 ± 1.3
$t\bar{t}$	5363 ± 48	12938 ± 81	7.1 ± 1.9	7.1 ± 1.9
Single top quark	269 ± 18	723 ± 31	–	–
W + jets	34 ± 5	36 ± 5	–	–
DY Zjj	152750 ± 510	394640 ± 880	273 ± 20	493 ± 31
Total backgrounds	159890 ± 510	411890 ± 890	283 ± 29	505 ± 43
EW Zjj signal	2833 ± 10	6665 ± 16	194.9 ± 2.6	379.7 ± 3.9
Data	163640	422499	418	892

η-ϕ plane, and (3) the p_{T} distribution function of the jet constituents, as defined in Ref. [58].

The variables are used as inputs to a likelihood discriminant on gluon and quark jets constructed from simulated dijet events. The performance of this QGL discriminant is evaluated and validated using independent, exclusive samples of Z + jet and dijet data [58]. Comparisons of simulation predictions and data distributions allow the derivation of corrections to the simulated QGL distributions and define a systematic uncertainty band.

4.2 Additional discriminating variables

An event balance variable, $R(p_{\mathrm{T}}^{\mathrm{hard}})$, is used to separate the signal from the background, defined as

$$R(p_{\mathrm{T}}^{\mathrm{hard}}) = \frac{|\vec{p}_{\mathrm{Tj_1}} + \vec{p}_{\mathrm{Tj_2}} + \vec{p}_{\mathrm{TZ}}|}{|\vec{p}_{\mathrm{Tj_1}}| + |\vec{p}_{\mathrm{Tj_2}}| + |\vec{p}_{\mathrm{TZ}}|} = \frac{|\vec{p}_{\mathrm{T}}^{\,\mathrm{hard}}|}{|\vec{p}_{\mathrm{Tj_1}}| + |\vec{p}_{\mathrm{Tj_2}}| + |\vec{p}_{\mathrm{TZ}}|}, \quad (1)$$

where $\vec{p}_{\mathrm{Tj_1}}$, $\vec{p}_{\mathrm{Tj_2}}$ and $\vec{p}_{\mathrm{TZ}}$ are, respectively, the transverse momenta of the two tagging jets and of the Z boson, and the numerator is the estimator of the p_{T} for the hard process, i.e. $p_{\mathrm{T}}^{\mathrm{hard}}$.

Angular variables useful for signal discrimination include the difference between the rapidity of the Z boson y_{Z} and the average rapidity of the two tagging jets, i.e.

$$y^* = y_{\mathrm{Z}} - \frac{1}{2}(y_{\mathrm{j_1}} + y_{\mathrm{j_2}}), \quad (2)$$

and the z^* Zeppenfeld variable [13] defined as

$$z^* = \frac{y^*}{\Delta y_{\mathrm{jj}}}. \quad (3)$$

The distributions for data and simulated samples of the m_{jj}, $R(p_{\mathrm{T}}^{\mathrm{hard}})$ and z^* variables, after the initial selection, are shown in Figs. 3 and 4, for the dielectron and dimuon channels, respectively. The distributions for data and simulated samples of the dijet transverse momentum (p_{Tjj}), pseudorapidity separation ($\Delta\eta_{\mathrm{jj}}$), and of the QGL output values of each jet, after the initial selection, are shown in Figs. 5 and 6, respectively, for the dielectron and dimuon channels. Good agreement between the data and the MC expectations is observed in both channels. In the lower panels of these plots the experimental uncertainties in the jet energy scales (JES) (dotted envelope) and the uncertainties due to the choice of QCD factorisation and normalization scales defined in Sect. 6 (dashed envelope) are shown.

5 Signal discriminants and extraction procedure

The EW Zjj signal is characterized by a large separation in pseudorapidity between the tagging jets, due to the small scattering-angle of the two initial partons. Because of both the topological configuration and the large energy of the outgoing partons, m_{jj} is also expected to be large. The evolution of $\Delta\eta_{\mathrm{jj}}$ with m_{jj} is expected to be different for signal and background events, and therefore these characteristics are expected to yield a high separation power between the EW Zjj and the DY Zjj productions. In addition, in signal events it is expected that the Z boson candidate is produced centrally in the rapidity region defined by the two tagging jets

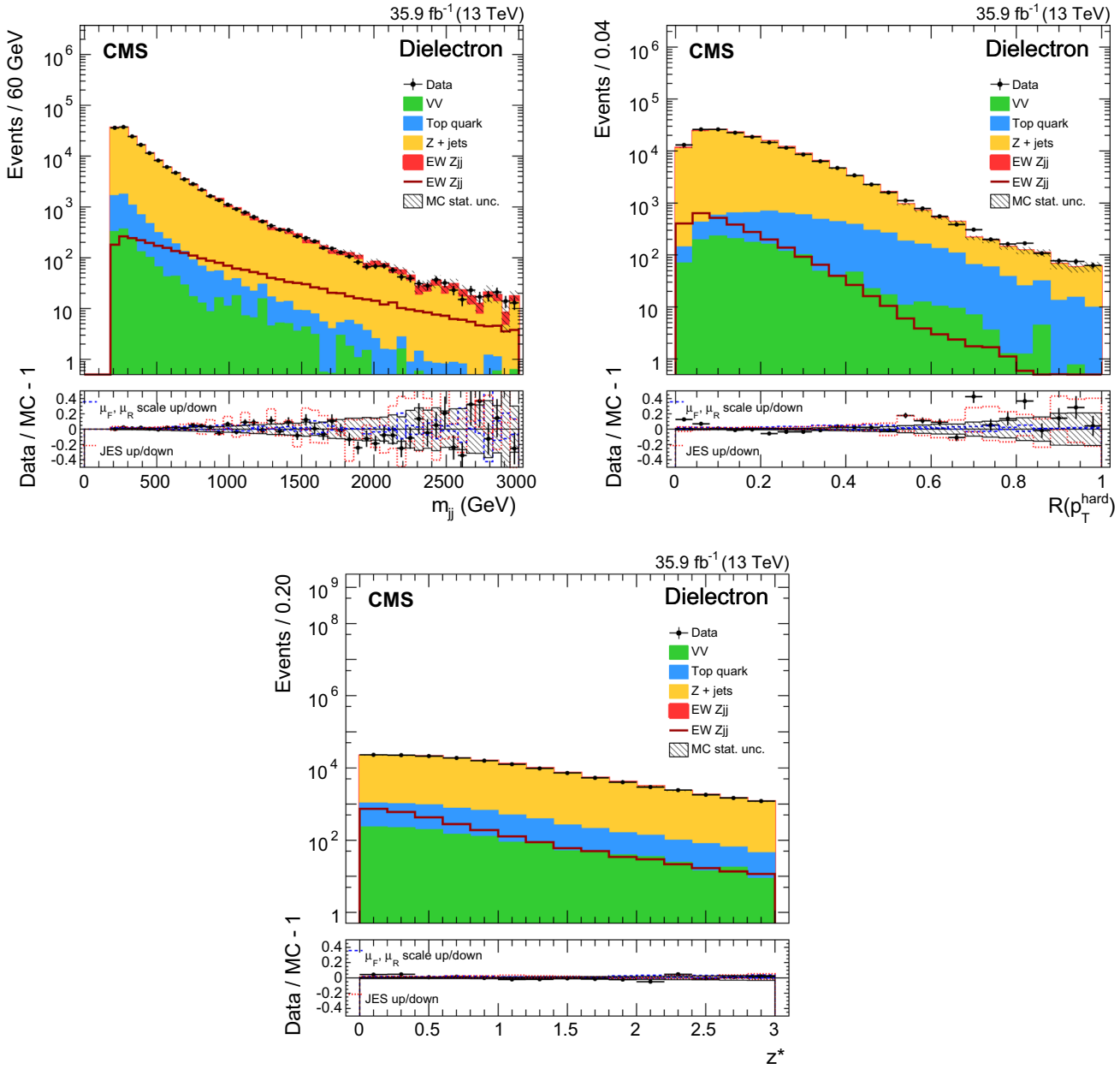


Fig. 3 Data and simulated event distributions for the dielectron event selection: m_{jj} (top left), $R(p_T^{hard})$ (top right), and z^* (bottom). The contributions from the different background sources and the signal are shown stacked, with data points superimposed. The expected signal-only contribution is also shown as an unfilled histogram. The lower panels show the relative difference between the data and expectations, as well as the uncertainty envelopes for JES and $\mu_{F,R}$ scale uncertainties

and that the Zjj system is approximately balanced in the transverse plane. As a consequence signal events are expected to yield lower values of both z^* and p_T^{hard} than the DY background. Other variables that are used to enhance the signal-to-background separation are related to the kinematics of the event (p_T, rapidity, and distance between the jets and/or the Z boson) or to the properties of the jets that are expected to be initiated by quarks. The variables that are used in the multivariate analysis are: (1) m_{jj}; (2) $\Delta\eta_{jj}$; (3) the dijet transverse momentum p_{Tjj}; (iv) the QGL values of the two tagging jets; (v) $R\left(p_T^{hard}\right)$ and z^*.

The output of the discriminator is built by training a boosted decision tree (BDT) from the TMVA package [59] to achieve an optimal separation between the EW Zjj and DY Zjj processes, independently in the dielectron and dimuon channels.

In order to improve the sensitivity for the extraction of the signal component, the transformation that originally projects

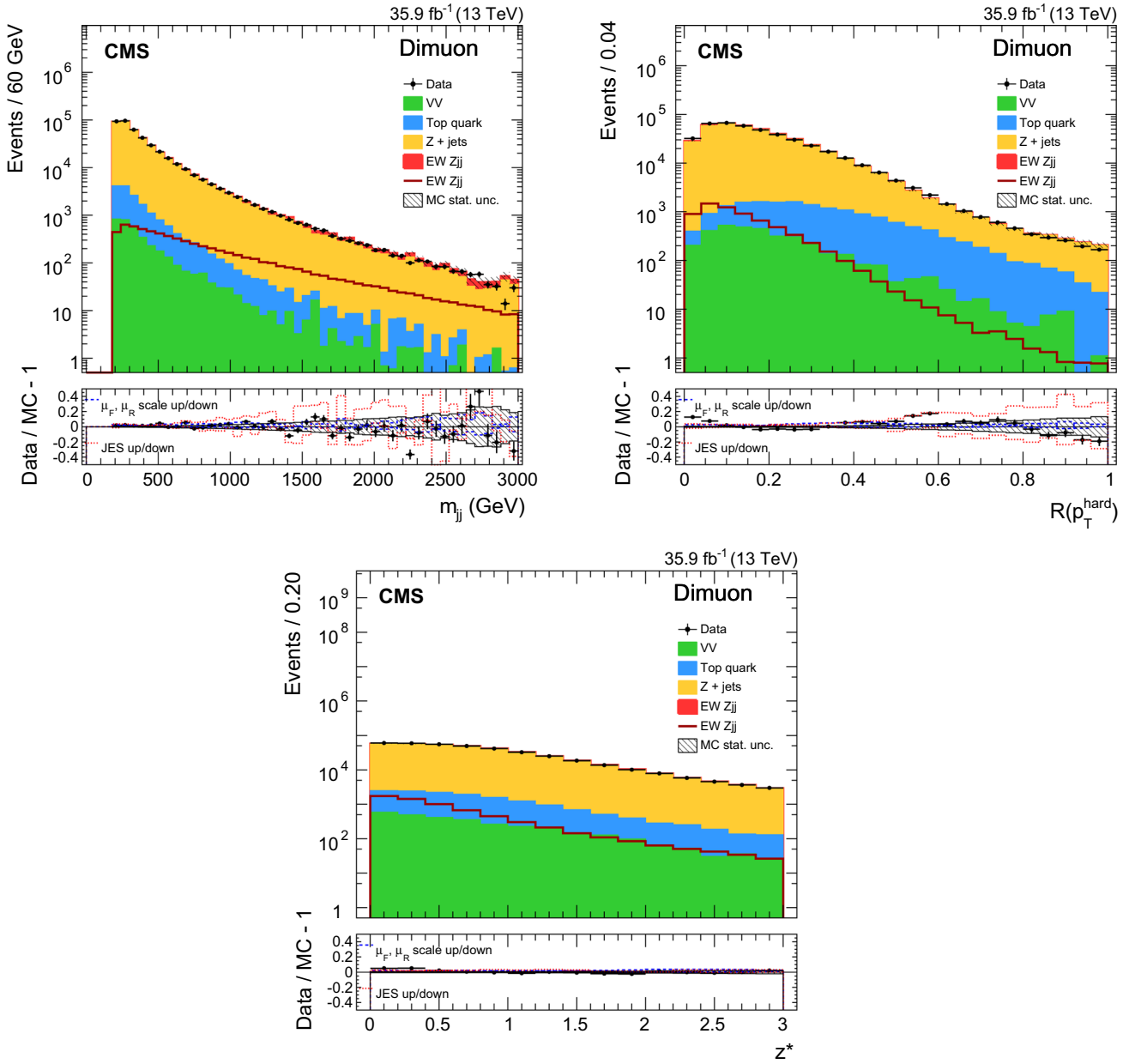


Fig. 4 Data and simulated event distributions for the dimuon event selection: m_{jj} (top left), $R(p_{\mathrm{T}}^{\mathrm{hard}})$ (top right), and z^* (bottom). The contributions from the different background sources and the signal are shown stacked, with data points superimposed. The expected signal-only contribution is also shown as an unfilled histogram. The lower panels show the relative difference between the data and expectations as well as the uncertainty envelopes for JES and $\mu_{\mathrm{F,R}}$ scale uncertainties

the BDT output value in the $[-1,+1]$ interval is changed into $\mathrm{BDT}' = \tanh^{-1}((\mathrm{BDT}+1)/2)$. This allows the purest signal region of the BDT output to be better sampled while keeping an equal-width binning of the BDT variable.

Figure 7 shows the distributions of the discriminants for the two leptonic channels. Good overall agreement between simulation and data is observed in all distributions, and the signal presence is visible at high BDT′ values.

A binned maximum likelihood calculation, which is used to fit simultaneously the strength modifiers for the EW Zjj and DY Zjj processes, $\mu = \sigma(\mathrm{EW\,Zjj})/\sigma_{\mathrm{LO}}(\mathrm{EW}\,\ell\ell\mathrm{jj})$ and $\upsilon = \sigma(\mathrm{DY})/\sigma_{\mathrm{th}}(\mathrm{DY})$, is built from the expected rates for each process. Nuisance parameters are added to modify the expected rates and shapes according to the estimate of the systematic uncertainties affecting the measurement.

The interference between the EW Zjj and DY Zjj processes is included in the fit procedure, and its strength scales

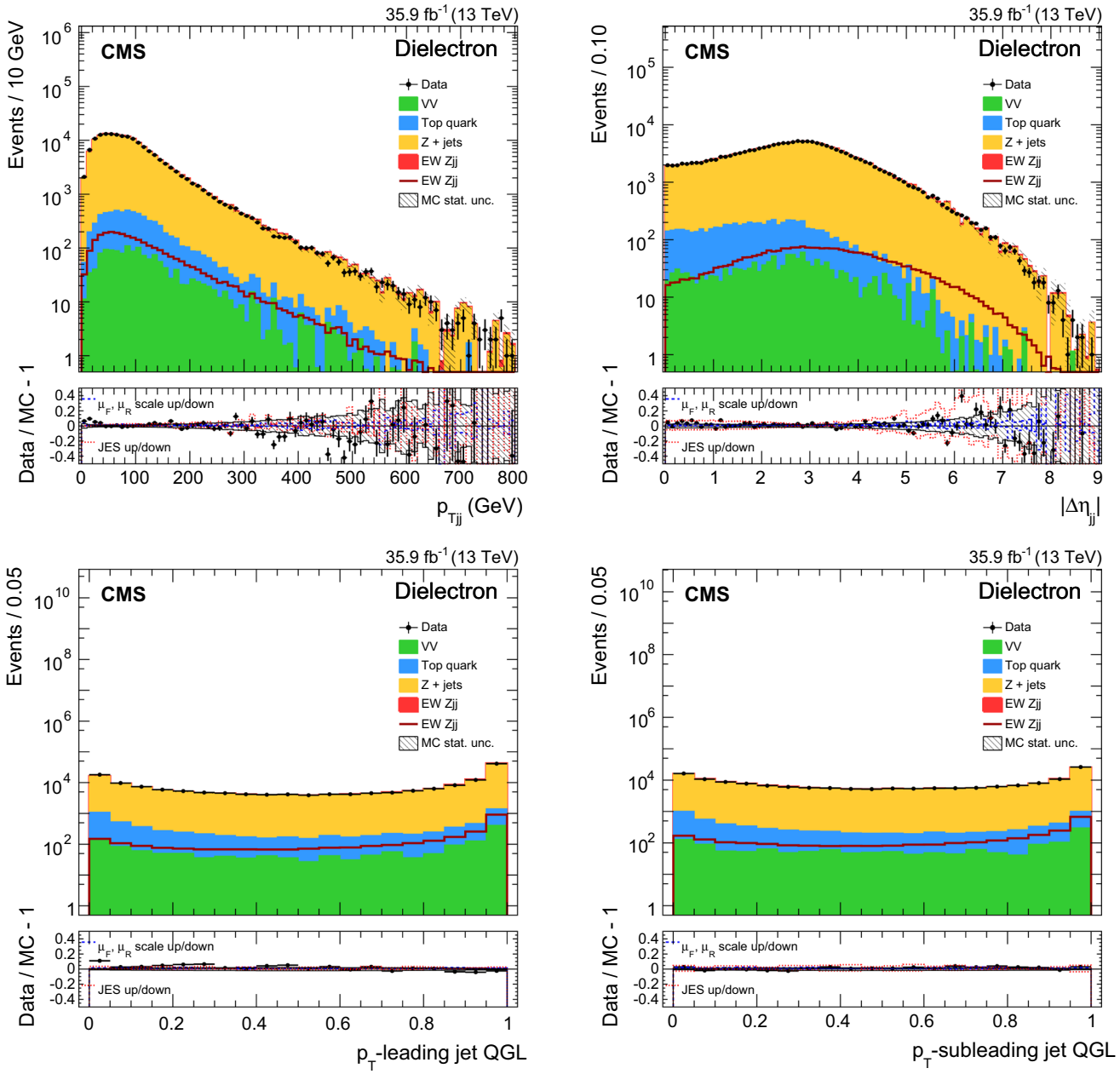


Fig. 5 Data and simulated event distributions for the dielectron event selection: dijet system transverse momentum (top left), dijet pseudorapidity opening (top right), p_{T}-leading jet QGL (bottom left), and p_{T}-subleading jet QGL (bottom right). The contributions from the different background sources and the signal are shown stacked, with data points superimposed. The expected signal-only contribution is also shown as an unfilled histogram. The lower panels show the relative difference between the data and expectations, as well as the uncertainty envelopes for JES and $\mu_{\mathrm{F,R}}$ scale uncertainties

as $\sqrt{\mu\upsilon}$. The interference model is derived from the MADGRAPH5_aMC@NLO simulation described in Section 3.

The parameters of the model (μ and υ) are determined by maximizing the likelihood. The statistical methodology follows the one used in other CMS analyses [6] using the asymptotic formulas [60]. In this procedure the systematic uncertainties affecting the measurement of the signal and background strengths (μ and υ) are constrained with log-normal probability distributions.

6 Systematic uncertainties

The main systematic uncertainties affecting the measurement are classified into experimental and theoretical sources. Some uncertainties affect only normalizations, while others affect both the normalization and shape of the BDT output distribution.

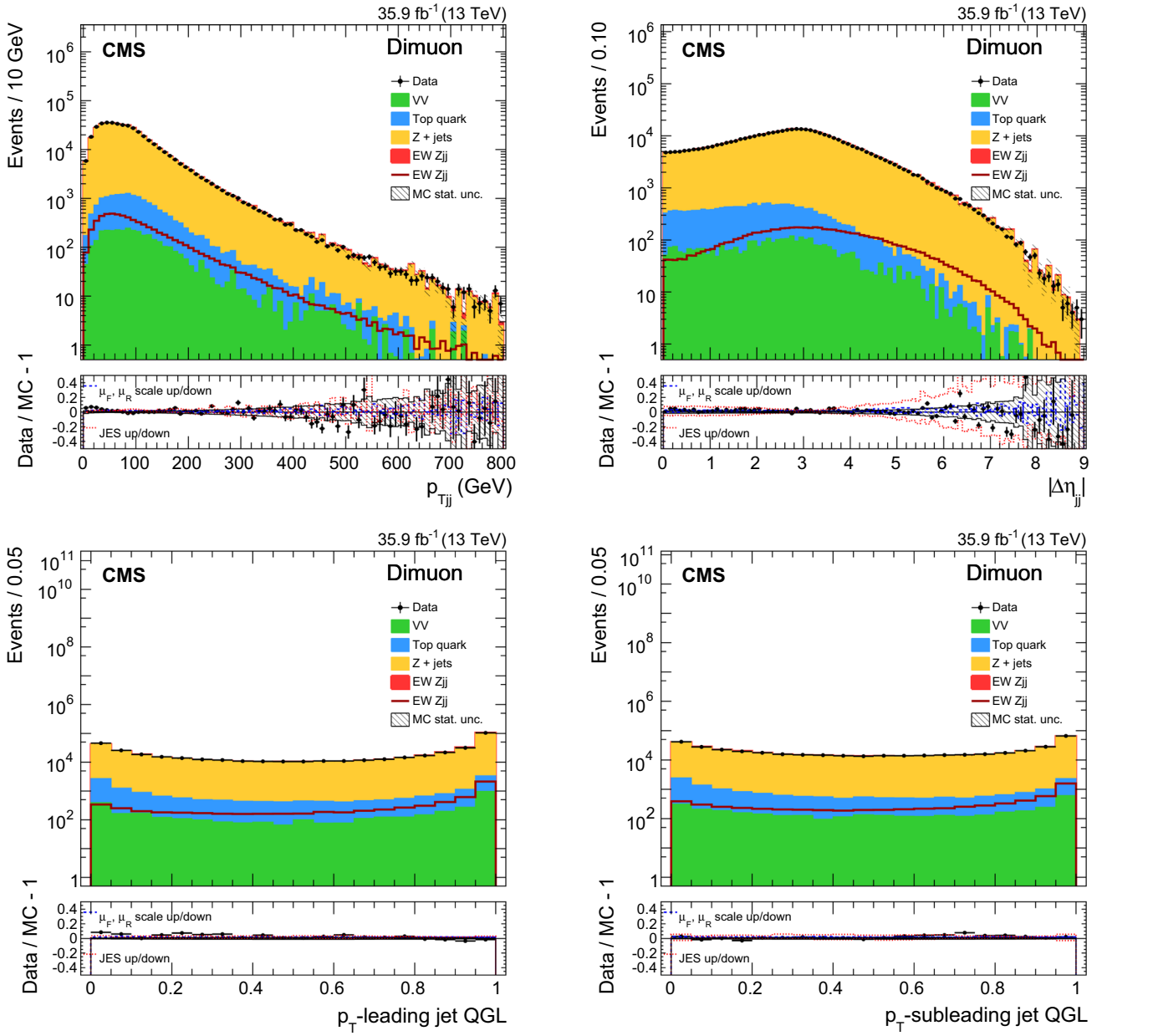


Fig. 6 Data and simulated event distributions for the dimuon event selection: dijet system transverse momentum (top left), dijet pseudorapidity opening (top right), p_{T}-leading jet QGL (bottom left), and p_{T}-subleading jet QGL (bottom right). The contributions from the different background sources and the signal are shown stacked, with data points superimposed. The expected signal-only contribution is also shown as an unfilled histogram. The lower panels show the relative difference between the data and expectations, as well as the uncertainty envelopes for JES and $\mu_{\mathrm{F,R}}$ scale uncertainties

6.1 Experimental uncertainties

The following experimental uncertainties are considered.

Integrated luminosity A 2.5% uncertainty is assigned to the value of the integrated luminosity [61].

Trigger and selection efficiencies Uncertainties in the efficiency corrections based on control samples in data for the leptonic trigger and offline selections amount to a total of 2–3%, depending on the lepton p_{T} and η for both the ee and $\mu\mu$ channels. These uncertainties are estimated by comparing the lepton efficiencies expected in simulation and measured in data with a tag-and-probe method [62].

Jet energy scale and resolution The energy of the jets enters at the selection level and in the computation of the kinematic variables used to calculate the discriminants. Therefore the uncertainty in the JES affects both the expected event

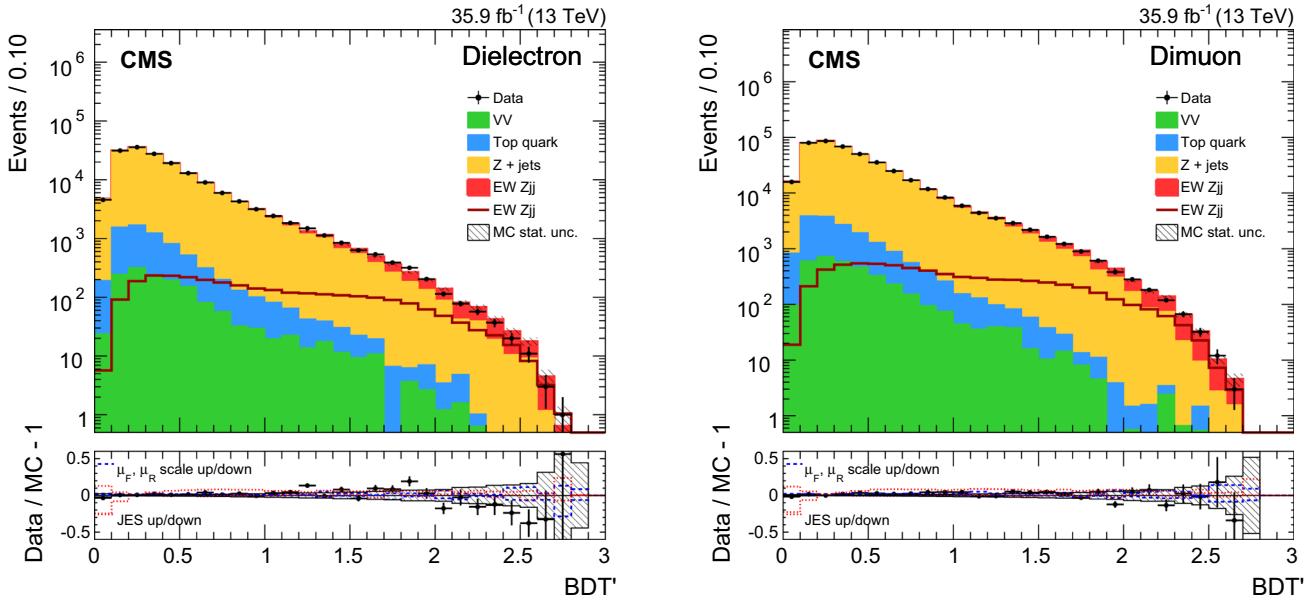


Fig. 7 Distributions for transformed BDT discriminants in dielectron (left) and dimuon (right) events. The contributions from the different background sources and the signal are shown stacked, with data points superimposed. The expected signal-only contribution is also shown as an unfilled histogram. The lower panels show the relative difference between the data and expectations, as well as the uncertainty envelopes for JES and $\mu_{F,R}$ scale uncertainties

yields and the final shapes. The effect of the JES uncertainty is studied by scaling up and down the reconstructed jet energy by p_T- and η-dependent scale factors [55]. An analogous approach is used for the JER. The final impact on the signal strength uncertainty amounts to about 3% for JES and 2% for JER.

QGL discriminator The uncertainty in the performance of the QGL discriminator is measured using independent Z + jet and dijet data [58]. Shape variations corresponding to the full data versus simulation differences are implemented. The variations are of the order of 10% for lower QGL output values, corresponding to gluon-like jets, and of the order of 5% for larger QGL output values, corresponding to quark-like jets. The final impact on the signal strength uncertainty amounts to about 1%.

Pileup Pileup can affect the identification and isolation of the leptons or the corrected energy of the jets. When jet clustering is performed, pileup can induce a distortion of the reconstructed dijet system because of the contamination from tracks and calorimetric deposits. This uncertainty is evaluated by generating alternative distributions of the number of pileup interactions, corresponding to a 5% uncertainty in the total inelastic pp cross section at $\sqrt{s} = 13\,\text{TeV}$.

Limited number of simulated events For each signal and background simulation, shape variations for the distributions are created by shifting each bin content up or down by its statistical uncertainty. This generates alternatives to the nominal shapes that are used to describe the uncertainty from the limited number of simulated events. Depending on the BDT output bin, the impact on the signal strength uncertainty can be up to 3%.

6.2 Theoretical uncertainties

The following theoretical uncertainties are considered in the analysis.

PDF The PDF uncertainties are evaluated by comparing the nominal distributions to those obtained when using the alternative PDFs of the NNPDF set, including α_S variations. The final impact on the signal strength uncertainty is less than 1%.

Factorization and renormalization scales To account for theoretical uncertainties, signal and background shape variations are built by changing the values of μ_F and μ_R from their defaults by factors of 2 or 1/2 in the ME calculation, simultaneously for μ_F and μ_R, but independently for each simulated sample. The final impact on the signal strength uncertainty amounts to 6% and 4% respectively for the signal and background variations.

Normalization of top quark and diboson backgrounds Diboson and top quark production processes are modelled with MC simulations. An uncertainty in the normalization of these backgrounds is assigned based on the PDF and μ_F, μ_R uncertainties, following calculations in Refs. [41,42,46]. The final impact on the signal strength uncertainty amounts to less than 1%.

Interference between EW Zjj *and* DY Zjj An overall normalization uncertainty and a shape uncertainty are assigned to the interference term in the fit, based on an envelope of prediction with different μ_F, μ_R scales. The final impact on the signal strength uncertainty amounts to 2–3%.

Parton showering model The uncertainty in the signal PS model and the event tune is assessed as the full difference of the acceptance and shape predictions using PYTHIA and HERWIG++. The final impact on the signal strength uncertainty amounts to about 4%.

The largest sources of experimental uncertainty come from the JES and the limited statistics of simulated events; the largest source of theoretical uncertainty comes from the μ_F, μ_R scale uncertainties.

7 Measurement of the EW Zjj production cross section

The signal strength, defined for the $\ell\ell$jj final state in the kinematic region described in Sect. 3, is extracted from the fit to the BDT output distribution as discussed in Sect. 5.

In the dielectron channel, the signal strength is measured to be

$$\begin{aligned}\mu &= 0.96 \pm 0.06\,(\text{stat}) \pm 0.13\,(\text{syst})\\ &= 0.96 \pm 0.14\,(\text{total}),\end{aligned}$$

corresponding to a measured signal cross section

$$\begin{aligned}\sigma(\text{EW } \ell\ell\text{jj}) &= 521 \pm 34\,(\text{stat}) \pm 68\,(\text{syst})\,\text{fb}\\ &= 521 \pm 76\,(\text{total})\,\text{fb}.\end{aligned}$$

In the dimuon channel, the signal strength is measured to be

$$\begin{aligned}\mu &= 0.97 \pm 0.04\,(\text{stat}) \pm 0.11\,(\text{syst})\\ &= 0.97 \pm 0.12\,(\text{total}),\end{aligned}$$

corresponding to a measured signal cross section

$$\begin{aligned}\sigma(\text{EW } \ell\ell\text{jj}) &= 524 \pm 23\,(\text{stat}) \pm 61\,(\text{syst})\,\text{fb}\\ &= 524 \pm 65\,(\text{total})\,\text{fb}.\end{aligned}$$

The results obtained for the different dilepton channels are compatible with each other, and in agreement with the SM predictions.

From the combined fit of the two channels, the signal strength is measured to be

$$\begin{aligned}\mu &= 0.98 \pm 0.04\,(\text{stat}) \pm 0.10\,(\text{syst})\\ &= 0.98 \pm 0.11\,(\text{total}),\end{aligned}$$

corresponding to a measured signal cross section

$$\begin{aligned}\sigma(\text{EW } \ell\ell\text{jj}) &= 534 \pm 20\,(\text{stat}) \pm 57\,(\text{syst})\,\text{fb}\\ &= 534 \pm 60\,(\text{total})\,\text{fb},\end{aligned}$$

in agreement with the SM prediction $\sigma_{\text{LO}}(\text{EW } \ell\ell\text{jj}) = 543 \pm 24\,\text{fb}$. In the combined fit, the DY strength is $\upsilon = 0.988 \pm 0.031$. Using the statistical methodology described in Ref. [60], the background-only hypotheses in the dielectron, dimuon, and combined channels are all excluded with significance well above 5σ.

8 Limits on anomalous gauge couplings

In the framework of EFT, new physics can be described as an infinite series of new interaction terms organized as an expansion in the mass dimension of the operators.

In the EW sector of the SM, the first higher-dimensional operators containing bosons are six-dimensional [15]:

$$\begin{aligned}\mathcal{O}_{WWW} &= \frac{c_{WWW}}{\Lambda^2} W_{\mu\nu} W^{\nu\rho} W^{\mu}_{\rho},\\ \mathcal{O}_{W} &= \frac{c_{W}}{\Lambda^2} (D^{\mu}\Phi)^{\dagger} W_{\mu\nu} (D^{\nu}\Phi),\\ \mathcal{O}_{B} &= \frac{c_{B}}{\Lambda^2} (D^{\mu}\Phi)^{\dagger} B_{\mu\nu} (D^{\nu}\Phi),\\ \widetilde{\mathcal{O}}_{WWW} &= \frac{\widetilde{c}_{WWW}}{\Lambda^2} \widetilde{W}_{\mu\nu} W^{\nu\rho} W^{\mu}_{\rho},\\ \widetilde{\mathcal{O}}_{W} &= \frac{\widetilde{c}_{W}}{\Lambda^2} (D^{\mu}\Phi)^{\dagger} \widetilde{W}_{\mu\nu} (D^{\nu}\Phi),\end{aligned} \tag{4}$$

where, as is customary, group indices are suppressed and the mass scale Λ is factorized from the coupling constants c. In Eq. (4), $W_{\mu\nu}$ is the SU(2) field strength, $B_{\mu\nu}$ is the U(1) field strength, Φ is the Higgs doublet, and operators with a tilde are the magnetic duals of the field strengths. The first three operators are charge and parity conserving, whereas the two last ones are not. In this paper, models with operators that preserve charge conjugation and parity symmetries can be included in the calculation either individually or in pairs. With these assumptions, the value of coupling constants divided by the mass scale c/Λ^2 are measured.

These operators have a rich phenomenology since they contribute to many multiboson scattering processes at tree level. The operator $\mathcal{O}_{WWW}$ modifies vertices with 3 to 6 vector bosons, whereas the operators $\mathcal{O}_W$ and $\mathcal{O}_B$ modify both HVV vertices and vertices with 3 or 4 vector bosons. A more detailed description of the phenomenology of these operators can be found in Ref. [63]. Modifications to the ZWW vertex are investigated in this case, since this modifies the pp $\rightarrow$ Zjj cross section.

Previously, modifications to these vertices have been studied using anomalous trilinear gauge couplings [64]. The rela-

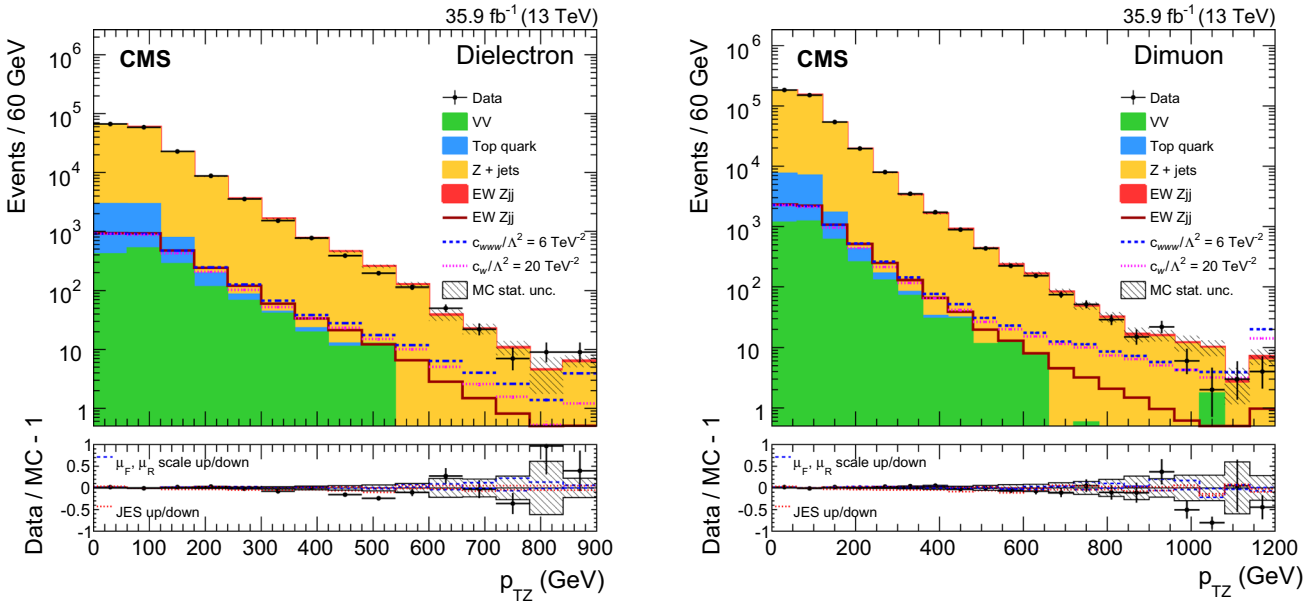


Fig. 8 Distributions of p_{TZ} in data and SM backgrounds, and various ATGC scenarios in the dielectron (left) and dimuon (right) channels

tionship between the dimension-6 operators in Eq. (4) and ATGCs can be found in Ref. [15].

8.1 ATGC signal simulation

ATGC signal events are simulated at LO using MADGRAPH5_aMC@NLO with the NNPDF3.0 PDF set for signal generation. Showering and hadronization of the events is performed with PYTHIA using the CUETP8M1 tune [28], using the same configuration as in the SM signal sample. The 'EWdim6NLO' model [15,24] is used for the generation of anomalous couplings.

For each event, 125 weights are assigned that correspond to a 5×5×5 grid in $c_{WWW}/\Lambda^2 \times c_W/\Lambda^2 \times c_B/\Lambda^2$. Equal bins are used in the interval $[-15, 15]\,\mathrm{TeV}^{-2}$ for c_{WWW}/Λ^2, $[-50, 50]\,\mathrm{TeV}^{-2}$ for c_W/Λ^2, and equal bins in the interval $[-500, 500]\,\mathrm{TeV}^{-2}$ for c_B/Λ^2.

8.2 Statistical analysis

The measurement of the coupling constants uses templates in the transverse momentum of the dilepton system (p_{TZ}). Because this is well-measured and longitudinally Lorentz invariant, this variable is robust against mismodelling and, in principle, ideal for this purpose. In the electron channel 15 equal bins for $0 < p_{\mathrm{TZ}} < 900\,\mathrm{GeV}$ are used, and 20 equal bins for $0 < p_{\mathrm{TZ}} < 1200\,\mathrm{GeV}$ are used in the muon channel, where the last bin contains overflow.

In order to construct the p_{TZ} templates, the associated weights calculated for each event are used to construct a parametrized model of the expected yield in each bin as a function of the values of the dimension-six operators' coupling constants. For each bin, the ratios of the expected signal yield with dimension-6 operators to the one without (leaving only the SM contribution) are fitted at each point of the grid to a quadratic polynomial. The highest bin is the one with the largest statistical power to detect the presence of higher dimensional operators. Figure 8 shows examples of the final templates, with the expected signal overlaid on the background expectation, for two different hypotheses of dimension-6 operators. The SM distribution is normalized to the expected cross section.

A simultaneous binned fit for the values of the ATGCs is performed in the two lepton channels. A profile likelihood method, the Wald Gaussian approximation and Wilks' theorem [60] are used to derive one-dimensional and two-dimensional limits at 95% confidence level (CL) on each of the three ATGC parameters and each combination of two ATGC parameters, respectively, while all other parameters are set to their SM values. Systematic and theoretical uncertainties are represented by individual nuisance parameters with log-normal distributions and are profiled in the fit.

8.3 Results

No significant deviation from the SM expectation is observed. Limits on ATGC parameters were previously set by LEP [65], ATLAS [66,67], and CMS [68,69]. The LHC semileptonic diboson analyses using 8 TeV data currently set the most stringent limits.

Table 2 One-dimensional limits on the ATGC EFT parameters at 95% CL

Coupling constant	Expected 95% CL interval (TeV^{-2})	Observed 95% CL interval (TeV^{-2})
c_{WWW}/Λ^2	$[-3.7, 3.6]$	$[-2.6, 2.6]$
c_W/Λ^2	$[-12.6, 14.7]$	$[-8.4, 10.1]$

Table 3 One-dimensional limits on the ATGC effective Lagrangian (LEP parametrization) parameters at 95% CL

Coupling constant	Expected 95% CL interval	Observed 95% CL interval
λ^Z	$[-0.014, 0.014]$	$[-0.010, 0.010]$
Δg_1^Z	$[-0.053, 0.061]$	$[-0.035, 0.042]$

Limits on the EFT parameters are reported and also translated into the equivalent parameters defined in an effective Lagrangian (LEP parametrization) in Ref. [70], without form factors: $\lambda^\gamma = \lambda^Z = \lambda$, $\Delta\kappa^Z = \Delta g_1^Z - \Delta\kappa^\gamma \tan^2\theta_W$. The parameters λ, $\Delta\kappa^Z$, and Δg_1^Z are considered, where the Δ symbols represents deviations from their respective SM values.

This analysis shows high sensitivity to c_{WWW}/Λ^2 and c_W/Λ^2 parameters (equivalently λ^Z and Δg_1^Z). The sensitivity to c_B/Λ^2 (equivalently $\Delta\kappa^Z$) parameter is very low since the contribution of this operator to the WWZ vertex is suppressed by the weak mixing angle.

Results for 1D limits on c_{WWW} and c_W (λ and Δg_1^Z) can be found in Table 2 (Table 3) respectively, and 2D limits are shown in Fig. 9. Results are dominated by the sensitivity in the muon channel due to the larger acceptance for muons. An ATGC signal is not included in the interference between EW and DY production. The effect on the limits is small (<3%).

9 Study of the hadronic and jet activity in Z + jet events

Now that the presence of an SM signal is established, the properties of the hadronic activity in the selected events can be examined. The production of additional jets in a region with a larger contribution from EW Zjj processes is explored in Sect. 9.1. Studies of the region in rapidity with expected low hadron activity (rapidity gap), using track-only observables, are presented in Sect. 9.2. Finally a study of hadronic activity vetoes, using both PF jets and track-only observables, is presented in Sect. 9.3. A significant suppression of the hadronic activity in signal events is expected because the final-state objects originate from pure electroweak interactions, in contrast with the radiative QCD production of jets in DY Zjj events. The reconstructed distributions are compared directly to the prediction obtained with a full simulation of the CMS detector.

In the following studies, event distributions are shown with a selection BDT $>$ 0.92, which allows a signal-enriched region to be selected with a similar fraction of signal and background events. The BDT $>$ 0.92 selection corresponds approximately to a selection BDT$'>$1.946 on the transformed BDT$'$ discriminants shown in Fig. 7.

9.1 Jet activity studies in a high-purity region

In this study, aside from the two tagging jets used in the preselection, all PF jets with a $p_T > 15$ GeV found within the pseudorapidity gap of the tagging jets, $\eta_{\text{min}}^{\text{tag jet}} < \eta < \eta_{\text{max}}^{\text{tag jet}}$, are used. The background contribution uses the normalizations obtained from the fit discussed in Sect. 7.

The p_T of the p_T-leading additional jet, as well as the scalar p_T sum (H_T) of all additional jets, are shown in Fig. 10. Data and expectations are generally in reasonable agreement for all distributions in the signal-enriched regions, with some

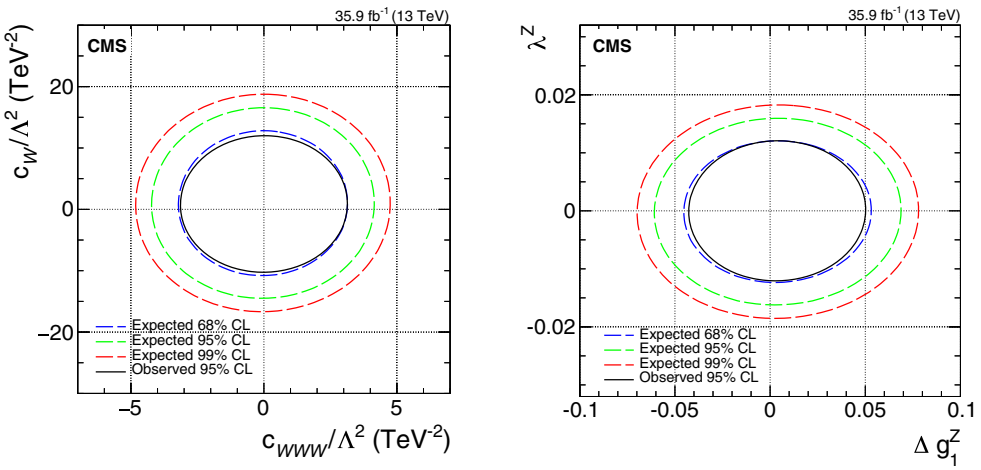


Fig. 9 Two-dimensional observed 95% CL limits (continuous black line) and expected 68, 95, and 99% CL limits on anomalous coupling parameters

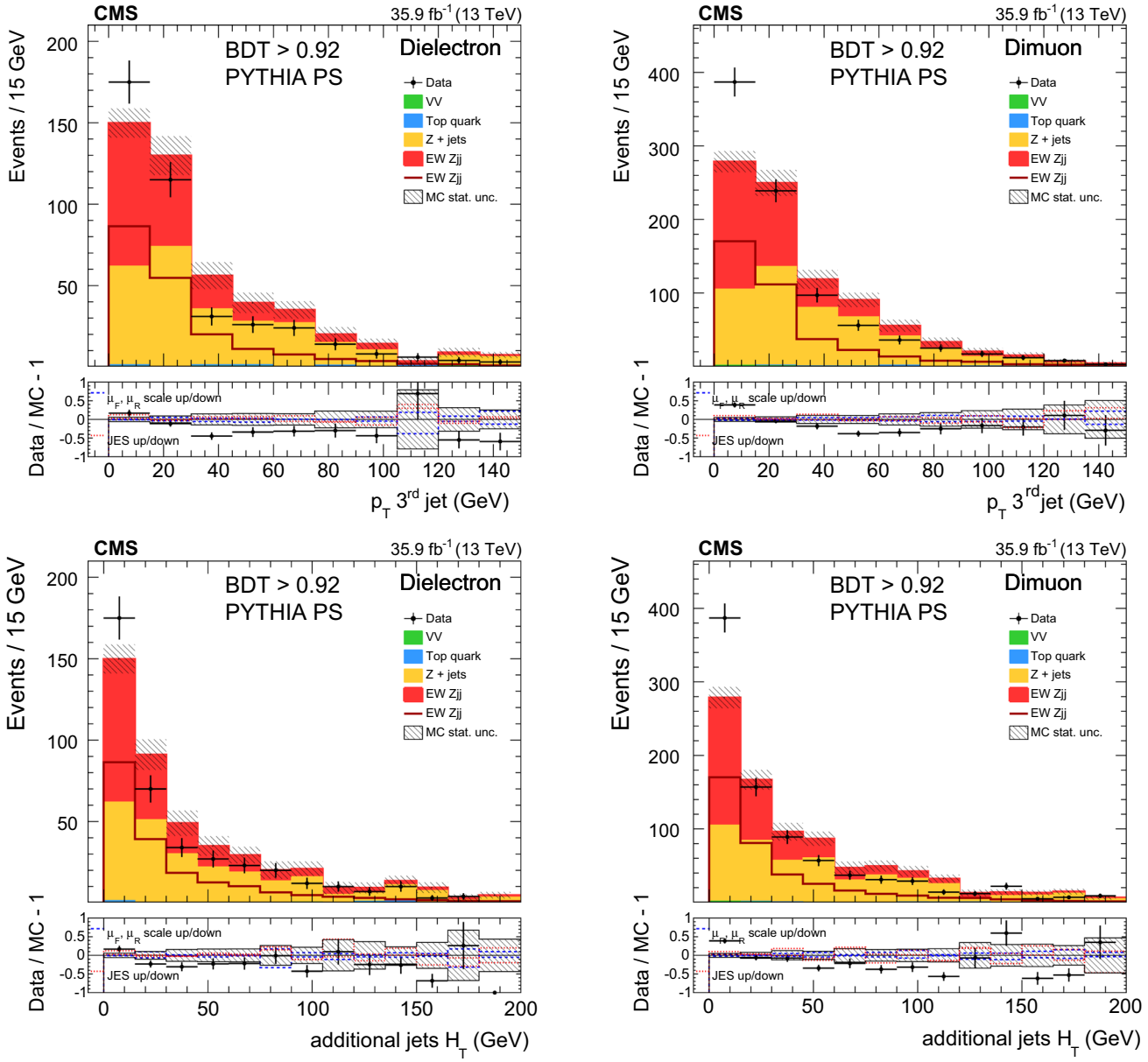


Fig. 10 Transverse momentum of the third highest p_{T} jet (top row), and H_{T} of all additional jets (bottom row) within the pseudorapidity interval of the two tagging jets in dielectron (left) and dimuon (right) events with BDT $>$ 0.92. The contributions from the different background sources and the signal are shown stacked, with data points superimposed. The expected signal-only contribution is also shown as an unfilled histogram. The lower panels show the relative difference between the data and expectations, as well as the uncertainty envelopes for JES and $\mu_{\mathrm{F,R}}$ scale uncertainties. In all distributions the first bin contains events where no additional jet with $p_{\mathrm{T}} > 15$ GeV is present

deficit of the simulation predictions for the rate of events with no additional jet activity. A suppression of the emission of additional jets is observed in data, when taking into account the background-only predictions. In the simulation of the signal, the additional jets are produced by the PS (see Sect. 3), so studying these distributions provides insight on the PS model in the rapidity-gap region.

9.2 Study of the charged-hadron activity

For this study, a collection is formed of high-purity tracks [71] with $p_{\mathrm{T}} > 0.3$ GeV that are uniquely associated with the main PV in the event. Tracks associated with the two leptons or with the tagging jets are excluded from the selection. The association between the selected tracks and the reconstructed PVs is carried out by minimizing the longitudinal impact parameter, which is defined as the z-distance between the

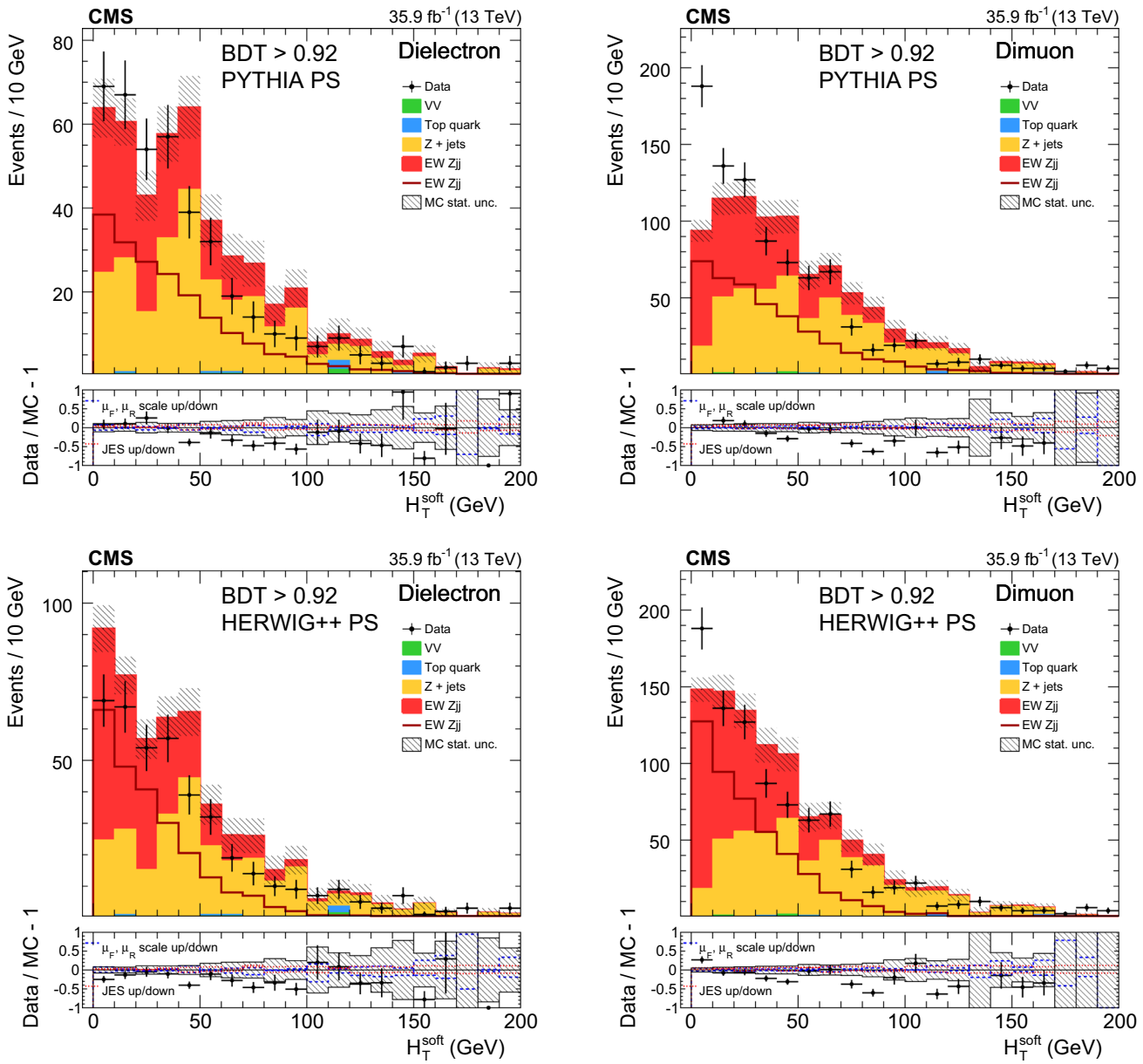
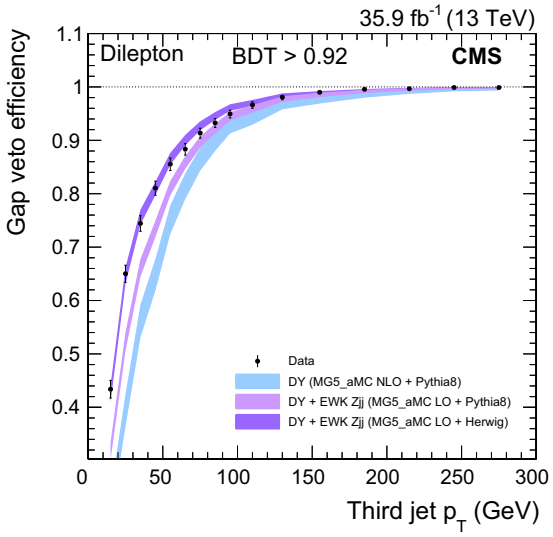


Fig. 11 H_{T} of additional soft track-jets with $p_{\mathrm{T}} > 1$ GeV in dielectron (left) and dimuon (right) events with BDT > 0.92. Data are compared to MC expectations with the PYTHIA PS model (top row), or the HERWIG++ PS model (bottom row). The contributions from the different background sources and the signal are shown stacked, with data points superimposed. The expected signal-only contribution is also shown as an unfilled histogram. The lower panels show the relative difference between the data and expectations, as well as the uncertainty envelopes for JES and $\mu_{\mathrm{F,R}}$ scale uncertainties

PV and the point of closest approach of the track helix to the PV, labelled d_z^{PV}. The association is required to satisfy $d_z^{\mathrm{PV}} < 2\,\mathrm{mm}$ and $d_z^{\mathrm{PV}} < 3\delta d_z^{\mathrm{PV}}$, where δd_z^{PV} is the uncertainty in d_z^{PV}.

A collection of "soft track jets" is defined by clustering the selected tracks using the anti-k_{T} clustering algorithm [51] with a distance parameter of $R = 0.4$. The use of track jets represents a clean and well-understood method [72] to reconstruct jets with energy as low as a few GeV. These jets are not affected by pileup because of the association of the constituent tracks with the hard-scattering vertex [73].

Track jets of low p_{T} and within $\eta_{\mathrm{min}}^{\mathrm{tag\,jet}} < \eta < \eta_{\mathrm{max}}^{\mathrm{tag\,jet}}$ are considered for the study of the central hadronic activity between the tagging jets. For each event, the scalar p_{T} sum of the soft-track jets with $p_{\mathrm{T}} > 1\,\mathrm{GeV}$ is computed, and referred to as "soft H_{T}". Figure 11 shows the distribution of the soft H_{T} in the signal-enriched region (BDT > 0.92), for



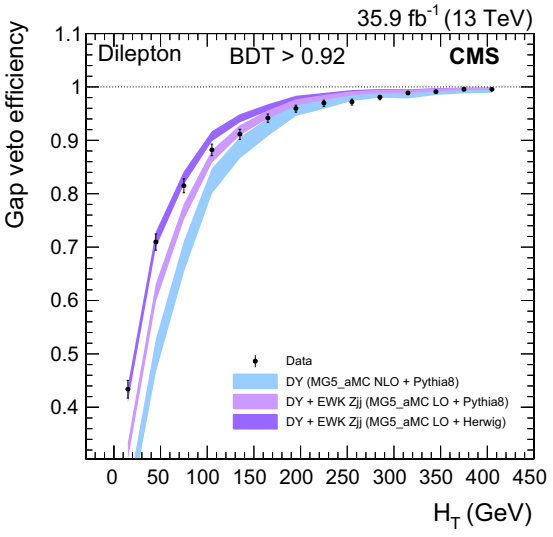
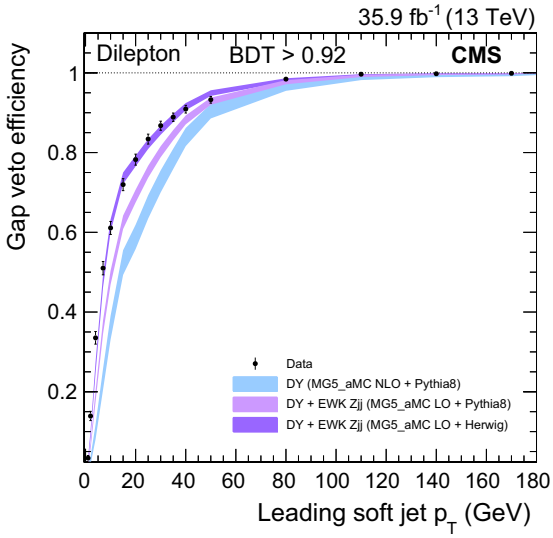


Fig. 12 Efficiency of a gap activity veto in dielectron and dimuon events with BDT $>$ 0.92, as a function of the additional jet p_{T} (left), and of the total H_{T} of additional jets (right). Data points are compared to MC expectations with only DY events, including signal with the PYTHIA PS model, or the HERWIG++ PS model. The bands represent the MC statistical uncertainty



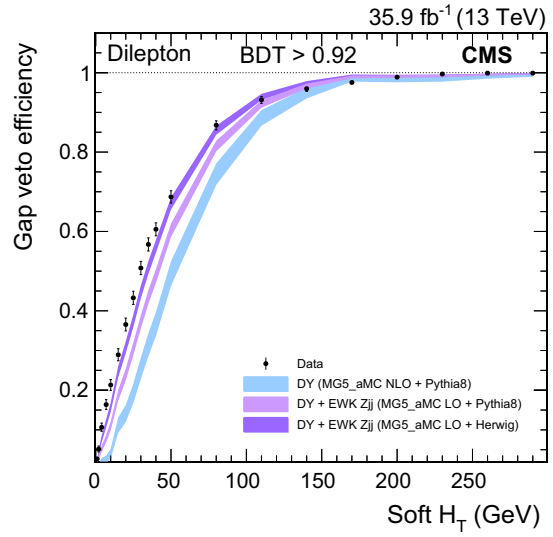


Fig. 13 Efficiency of a gap activity veto in dielectron and dimuon events with BDT $>$ 0.92, as a function of the leading soft track-jet p_{T} (left), and of the total soft H_{T} (right). Data points are compared to MC expectations with only DY events, including signal with the PYTHIA PS model, or the HERWIG++ PS model. The bands represent the MC statistical uncertainty

the dielectron and dimuon channels, compared to predictions from PYTHIA and HERWIG++ PS models.

Overall, a reasonable agreement is observed between data and the simulation.

9.3 Study of gap activity vetoes

The efficiency of a gap activity veto corresponds to the fraction of events with a measured gap activity below a given threshold. This efficiency can be studied as a function of the applied threshold, and for different gap activity observables. The veto thresholds studied here start at 15 GeV for gap activities measured with standard PF jets, while they go down to 1 GeV for gap activities measured with soft track jets.

Figure 12 shows the gap activity veto efficiency of combined dielectron and dimuon events in the signal-enriched region when placing an upper threshold on the p_{T} of the additional third jet, or on the total H_{T} of all additional jets. The observed efficiency in data is compared to expected efficiencies for background-only events, and efficiencies for back-

ground plus signal events where the signal is modeled with PYTHIA or HERWIG++. Data points disfavour the background-only predictions and are in reasonable agreement with the presence of the signal for both PS predictions.

Figure 13 shows the gap activity veto efficiency of combined dielectron and dimuon events in the signal-enriched region when placing an upper threshold on the p_{T} of the leading soft jet, or on the total soft H_{T}. The data points disfavour the background-only predictions and are in reasonable agreement with the presence of the signal with both PS predictions. Comparisons between the signal gap activity predictions obtained with PYTHIA PS model and the HERWIG++ PS model have been previously studied [13], and are consistent with the predictions found here. Among the two considered signal models, the data seem to prefer the signal model with HERWIG++ PS at low gap activity values, whereas the PYTHIA (v8.212) PS predictions seem to be preferred by the data in the case of larger gap activities.

10 Summary

The cross section for the electroweak (EW) production of a Z boson in association with two jets in the $\ell\ell$jj final state is measured in proton-proton collisions at $\sqrt{s} = 13\,\mathrm{TeV}$ in the kinematic region defined by $m_{\ell\ell} > 50\,\mathrm{GeV}$, $m_{\mathrm{jj}} > 120\,\mathrm{GeV}$, and transverse momenta $p_{\mathrm{Tj}} > 25\,\mathrm{GeV}$. The result

$$\sigma(\mathrm{EW}\ \ell\ell\mathrm{jj}) = 534 \pm 20\,(\mathrm{stat}) \pm 57\,(\mathrm{syst})\,\mathrm{fb},$$

agrees with the standard model prediction.

The increased cross section and integrated luminosity recorded at 13 TeV, as well as the more precise NLO modelling of background processes, have led to a more precise measurement of the EW Zjj process, relative to earlier CMS and ATLAS results, where the relative precision was approximately 20% [3,4,16,17].

No evidence for anomalous trilinear gauge couplings is found. The following one-dimensional limits at 95% CL are obtained: $-2.6 < c_{WWW}/\Lambda^2 < 2.6\,\mathrm{TeV}^{-2}$ and $-8.4 < c_W/\Lambda^2 < 10.1\,\mathrm{TeV}^{-2}$. These results provide the most stringent constraints on c_{WWW} to date.

In events from a signal-enriched region, the additional hadron activity is also studied, as well as the efficiencies for a gap-activity veto, and generally good agreement is found between data and quantum chromodynamics predictions with either the PYTHIA or HERWIG++ parton shower and hadronization model.

Acknowledgements We congratulate our colleagues in the CERN accelerator departments for the excellent performance of the LHC and thank the technical and administrative staffs at CERN and at other CMS institutes for their contributions to the success of the CMS effort. In addition, we gratefully acknowledge the computing centers and personnel of the Worldwide LHC Computing Grid for delivering so effectively the computing infrastructure essential to our analyses. Finally, we acknowledge the enduring support for the construction and operation of the LHC and the CMS detector provided by the following funding agencies: the Austrian Federal Ministry of Science, Research and Economy and the Austrian Science Fund; the Belgian Fonds de la Recherche Scientifique, and Fonds voor Wetenschappelijk Onderzoek; the Brazilian Funding Agencies (CNPq, CAPES, FAPERJ, and FAPESP); the Bulgarian Ministry of Education and Science; CERN; the Chinese Academy of Sciences, Ministry of Science and Technology, and National Natural Science Foundation of China; the Colombian Funding Agency (COLCIENCIAS); the Croatian Ministry of Science, Education and Sport, and the Croatian Science Foundation; the Research Promotion Foundation, Cyprus; the Secretariat for Higher Education, Science, Technology and Innovation, Ecuador; the Ministry of Education and Research, Estonian Research Council via IUT23-4 and IUT23-6 and European Regional Development Fund, Estonia; the Academy of Finland, Finnish Ministry of Education and Culture, and Helsinki Institute of Physics; the Institut National de Physique Nucléaire et de Physique des Particules / CNRS, and Commissariat à l'Énergie Atomique et aux Énergies Alternatives / CEA, France; the Bundesministerium für Bildung und Forschung, Deutsche Forschungsgemeinschaft, and Helmholtz-Gemeinschaft Deutscher Forschungszentren, Germany; the General Secretariat for Research and Technology, Greece; the National Scientific Research Foundation, and National Innovation Office, Hungary; the Department of Atomic Energy and the Department of Science and Technology, India; the Institute for Studies in Theoretical Physics and Mathematics, Iran; the Science Foundation, Ireland; the Istituto Nazionale di Fisica Nucleare, Italy; the Ministry of Science, ICT and Future Planning, and National Research Foundation (NRF), Republic of Korea; the Lithuanian Academy of Sciences; the Ministry of Education, and University of Malaya (Malaysia); the Mexican Funding Agencies (BUAP, CINVESTAV, CONACYT, LNS, SEP, and UASLP-FAI); the Ministry of Business, Innovation and Employment, New Zealand; the Pakistan Atomic Energy Commission; the Ministry of Science and Higher Education and the National Science Centre, Poland; the Fundação para a Ciência e a Tecnologia, Portugal; JINR, Dubna; the Ministry of Education and Science of the Russian Federation, the Federal Agency of Atomic Energy of the Russian Federation, Russian Academy of Sciences, the Russian Foundation for Basic Research and the Russian Competitiveness Program of NRNU "MEPhI"; the Ministry of Education, Science and Technological Development of Serbia; the Secretaría de Estado de Investigación, Desarrollo e Innovación, Programa Consolider-Ingenio 2010, Plan de Ciencia, Tecnología e Innovación 2013-2017 del Principado de Asturias and Fondo Europeo de Desarrollo Regional, Spain; the Swiss Funding Agencies (ETH Board, ETH Zurich, PSI, SNF, UniZH, Canton Zurich, and SER); the Ministry of Science and Technology, Taipei; the Thailand Center of Excellence in Physics, the Institute for the Promotion of Teaching Science and Technology of Thailand, Special Task Force for Activating Research and the National Science and Technology Development Agency of Thailand; the Scientific and Technical Research Council of Turkey, and Turkish Atomic Energy Authority; the National Academy of Sciences of Ukraine, and State Fund for Fundamental Researches, Ukraine; the Science and Technology Facilities Council, UK; the US Department of Energy, and the US National Science Foundation. Individuals have received support from the Marie-Curie program and the European Research Council and Horizon 2020 Grant, contract No. 675440 (European Union); the Leventis Foundation; the A. P. Sloan Foundation; the Alexander von Humboldt Foundation; the Belgian Federal Science Policy Office; the Fonds pour la Formation à la Recherche dans l'Industrie et dans l'Agriculture (FRIA-Belgium); the Agentschap voor Innovatie door Wetenschap en Technologie (IWT-Belgium); the Ministry of Education, Youth and Sports (MEYS) of the Czech Republic; the Council of Scientific and Industrial Research, India; the HOMING PLUS program of the Foundation for Polish Science, cofinanced from European Union, Regional

Development Fund, the Mobility Plus program of the Ministry of Science and Higher Education, the National Science Center (Poland), contracts Harmonia 2014/14/M/ST2/00428, Opus 2014/13/B/ST2/02543, 2014/15/B/ST2/03998, and 2015/19/B/ST2/02861, Sonata-bis 2012/07/E/ST2/01406; the National Priorities Research Program by Qatar National Research Fund; the Programa Severo Ochoa del Principado de Asturias; the Thalis and Aristeia programs cofinanced by EU-ESF and the Greek NSRF; the Rachadapisek Sompot Fund for Postdoctoral Fellowship, Chulalongkorn University and the Chulalongkorn Academic into Its 2nd Century Project Advancement Project (Thailand); the Welch Foundation, contract C-1845; and the Weston Havens Foundation (USA).

Open Access This article is distributed under the terms of the Creative Commons Attribution 4.0 International License (http://creativecommons.org/licenses/by/4.0/), which permits unrestricted use, distribution, and reproduction in any medium, provided you give appropriate credit to the original author(s) and the source, provide a link to the Creative Commons license, and indicate if changes were made.
Funded by SCOAP[3].

References

1. C. Oleari, D. Zeppenfeld, QCD corrections to electroweak $\ell\nu_\ell$jj and $\ell^+\ell^-$jj production. Phys. Rev. D **69**, 093004 (2004). https://doi.org/10.1103/PhysRevD.69.093004. arXiv:hep-ph/0310156
2. H. Chehime, D. Zeppenfeld, Single W and Z boson production as a probe for rapidity gaps at the SSC. Phys. Rev. D **47**, 3898 (1993). https://doi.org/10.1103/PhysRevD.47.3898
3. CMS Collaboration, Measurement of the hadronic activity in events with a Z and two jets and extraction of the cross section for the electroweak production of a Z with two jets in pp collisions at $\sqrt{s} = 7$ TeV. JHEP **10** 062, (2013). https://doi.org/10.1007/JHEP10(2013)062. arXiv:1305.7389
4. CMS Collaboration, Measurement of electroweak production of two jets in association with a Z boson in proton-proton collisions at $\sqrt{s} = 8$ TeV. Eur. Phys. J. C **75** 66, (2015). https://doi.org/10.1140/epjc/s10052-014-3232-5. arXiv:1410.3153
5. ATLAS Collaboration, Observation of a new particle in the search for the Standard Model Higgs boson with the ATLAS detector at the LHC. Phys. Lett. B **716** 1, (2012). https://doi.org/10.1016/j.physletb.2012.08.020. arXiv:1207.7214
6. CMS Collaboration, Observation of a new boson at a mass of 125 GeV with the CMS experiment at the LHC. Phys. Lett. B **716** 30, (2012). https://doi.org/10.1016/j.physletb.2012.08.021. arXiv:1207.7235
7. CMS Collaboration, Observation of a new boson with mass near 125 GeV in pp collisions at $\sqrt{s} = 7$ and 8 TeV. JHEP **06** 081, (2013). https://doi.org/10.1007/JHEP06(2013)081. arXiv:1303.4571
8. G.-C. Cho et al., Weak boson fusion production of supersymmetric particles at the CERN LHC. Phys. Rev. D **73**, 054002 (2006). https://doi.org/10.1103/PhysRevD.73.054002. arXiv:hep-ph/0601063
9. B. Dutta et al., Vector boson fusion processes as a probe of supersymmetric electroweak sectors at the LHC. Phys. Rev. D **87**, 035029 (2013). https://doi.org/10.1103/PhysRevD.87.035029. arXiv:1210.0964
10. CMS Collaboration, Search for supersymmetry in the vector-boson fusion topology in proton-proton collisions at $\sqrt{s} = 8$ TeV. JHEP **11** 189, (2015). https://doi.org/10.1007/JHEP11(2015)189. arXiv:1508.07628
11. CMS Collaboration, Search for dark matter and supersymmetry with a compressed mass spectrum in the vector boson fusion topology in proton-proton collisions at $\sqrt{s} = 8$ TeV. Phys. Rev. Lett. **118** 021802, (2017). https://doi.org/10.1103/PhysRevLett.118.021802. arXiv:1605.09305
12. J.D. Bjorken, Rapidity gaps and jets as a new physics signature in very high-energy hadron hadron collisions. Phys. Rev. D **47**, 101 (1993). https://doi.org/10.1103/PhysRevD.47.101
13. F. Schissler, D. Zeppenfeld, Parton shower effects on W and Z production via vector boson fusion at NLO QCD. JHEP **04**, 057 (2013). https://doi.org/10.1007/JHEP04(2013)057. arXiv:1302.2884
14. K. Hagiwara, S. Ishihara, R. Szalapski, D. Zeppenfeld, Low-energy effects of new interactions in the electroweak boson sector. Phys. Rev. D **48**, 2182 (1993). https://doi.org/10.1103/PhysRevD.48.2182
15. C. Degrande et al., Effective field theory: a modern approach to anomalous couplings. Ann. Phys. **335**, 21 (2013). https://doi.org/10.1016/j.aop.2013.04.016. arXiv:1205.4231
16. ATLAS Collaboration, Measurement of the electroweak production of dijets in association with a Z-boson and distributions sensitive to vector boson fusion in proton-proton collisions at $\sqrt{s} = 8$ TeV using the ATLAS detector. JHEP **04** 031, (2014). https://doi.org/10.1007/JHEP04(2014)031. arXiv:1401.7610
17. ATLAS Collaboration, Measurement of the cross-section for electroweak production of dijets in association with a Z boson in pp collisions at $\sqrt{s} = 13$ TeV with the ATLAS detector. Phys. Lett.B **775** 206, (2017). https://doi.org/10.1016/j.physletb.2017.10.040. arXiv:1709.10264
18. CMS Collaboration, Description and performance of track and primary-vertex reconstruction with the CMS tracker. JINST **9** P10009, (2014). https://doi.org/10.1088/1748-0221/9/10/P10009. arXiv:1405.6569
19. CMS Collaboration, Performance of electron reconstruction and selection with the CMS detector in proton-proton collisions at $\sqrt{s} = 8$ TeV. JINST **10** P06005, (2015). https://doi.org/10.1088/1748-0221/10/06/P06005. arXiv:1502.02701
20. CMS Collaboration, Performance of CMS muon reconstruction in pp collision events at $\sqrt{s} = 7$ TeV. JINST **7** P10002, (2012). https://doi.org/10.1088/1748-0221/7/10/P10002. arXiv:1206.4071
21. CMS Collaboration, Particle-flow reconstruction and global event description with the CMS detector. JINST **12** P10003, (2017). https://doi.org/10.1088/1748-0221/12/10/P10003. arXiv:1706.04965
22. CMS Collaboration, The CMS experiment at the CERN LHC. JINST **3** S08004, (2008). https://doi.org/10.1088/1748-0221/3/08/S08004
23. J. Alwall et al., MadGraph 5: going beyond. JHEP **06**, 128 (2011). https://doi.org/10.1007/JHEP06(2011)128. arXiv:1106.0522
24. J. Alwall et al., The automated computation of tree-level and next-to-leading order differential cross sections, and their matching to parton shower simulations. JHEP **07**, 079 (2014). https://doi.org/10.1007/JHEP07(2014)079. arXiv:1405.0301
25. T. Sjöstrand, S. Mrenna, P. Skands, A brief introduction to PYTHIA 8.1. Comput. Phys. Commun. **178**, 852 (2008). https://doi.org/10.1016/j.cpc.2008.01.036. arXiv:0710.3820
26. T. Sjöstrand et al., An introduction to PYTHIA 8.2. Comput. Phys. Commun. **191**, 159 (2015). https://doi.org/10.1016/j.cpc.2015.01.024. arXiv:1410.3012
27. NNPDF Collaboration, Parton distributions for the LHC Run II. JHEP **04** 040, (2015). https://doi.org/10.1007/JHEP04(2015)040. arXiv:1410.8849
28. CMS Collaboration, Event generator tunes obtained from underlying event and multiparton scattering measurements. Eur. Phys. J. C **76** 155, (2016). https://doi.org/10.1140/epjc/s10052-016-3988-x. arXiv:1512.00815
29. K. Arnold et al., VBFNLO: a parton level Monte Carlo for processes with electroweak bosons. Comput. Phys. Com-

mun. **180**, 1661 (2009). https://doi.org/10.1016/j.cpc.2009.03.006. arXiv:0811.4559
30. J. Baglio et al., VBFNLO: a parton level Monte Carlo for processes with electroweak bosons—manual for version 2.7.0. (2011). arXiv:1107.4038
31. K. Arnold et al., Release note—VBFNLO-2.6.0. (2012). arXiv:1207.4975
32. M. Bähr et al., Herwig++ physics and manual. Eur. Phys. J. C **58**, 639 (2008). https://doi.org/10.1140/epjc/s10052-008-0798-9. arXiv:0803.0883
33. M.H. Seymour, A. Siodmok, Constraining MPI models using σ_{eff} and recent Tevatron and LHC underlying event data. JHEP **10**, 113 (2013). https://doi.org/10.1007/JHEP10(2013)113. arXiv:1307.5015
34. R. Frederix, S. Frixione, Merging meets matching in MC@NLO. JHEP **12**, 061 (2012). https://doi.org/10.1007/JHEP12(2012)061. arXiv:1209.6215
35. M.L. Mangano, M. Moretti, F. Piccinini, M. Treccani, Matching matrix elements and shower evolution for top-quark production in hadronic collisions. JHEP **01**, 013 (2007). https://doi.org/10.1088/1126-6708/2007/01/013. arXiv:hep-ph/0611129
36. J. Alwall et al., Comparative study of various algorithms for the merging of parton showers and matrix elements in hadronic collisions. Eur. Phys. J. C **53**, 473 (2008). https://doi.org/10.1140/epjc/s10052-007-0490-5. arXiv:0706.2569
37. K. Melnikov, F. Petriello, Electroweak gauge boson production at hadron colliders through $\mathcal{O}(\alpha_S^2)$. Phys. Rev. D **74**, 114017 (2006). https://doi.org/10.1103/PhysRevD.74.114017. arXiv:hep-ph/0609070
38. P. Nason, A new method for combining NLO QCD with shower Monte Carlo algorithms. JHEP **11**, 040 (2004). https://doi.org/10.1088/1126-6708/2004/11/040. arXiv:hep-ph/0409146
39. S. Frixione, P. Nason, C. Oleari, Matching NLO QCD computations with parton shower simulations: the POWHEG method. JHEP **11**, 070 (2007). https://doi.org/10.1088/1126-6708/2007/11/070. arXiv:0709.2092
40. S. Alioli, P. Nason, C. Oleari, E. Re, A general framework for implementing NLO calculations in shower Monte Carlo programs: the POWHEG BOX. JHEP **06**, 043 (2010). https://doi.org/10.1007/JHEP06(2010)043. arXiv:1002.2581
41. N. Kidonakis, Differential and total cross sections for top pair and single top production. in *Proceedings of the XX International Workshop on Deep-Inelastic Scattering and Related Subjects*. Bonn, Germany (2012). https://doi.org/10.3204/DESY-PROC-2012-02/251. arXiv:1205.3453
42. M. Czakon, P. Fiedler, A. Mitov, Total top-quark pair-production cross section at hadron colliders through $\mathcal{O}(\alpha_S^4)$. Phys. Rev. Lett. **110**, 252004 (2013). https://doi.org/10.1103/PhysRevLett.110.252004. arXiv:1303.6254
43. S. Alioli, P. Nason, C. Oleari, E. Re, NLO single-top production matched with shower in POWHEG: s- and t-channel contributions. JHEP **09**, 111 (2009). https://doi.org/10.1088/1126-6708/2009/09/111. arXiv:0907.4076. [Erratum: 10.1007/JHEP02(2010)011]
44. E. Re, Single-top Wt-channel production matched with parton showers using the POWHEG method. Eur. Phys. J. C **71**, 1547 (2011). https://doi.org/10.1140/epjc/s10052-011-1547-z. arXiv:1009.2450
45. N. Kidonakis, Top quark production, in *Proceedings, Helmholtz International Summer School on Physics of Heavy Quarks and Hadrons (HQ 2013): JINR*, Dubna, Russia, July 15–28, 2013, p. 139. (2014). https://doi.org/10.3204/DESY-PROC-2013-03/Kidonakis. arXiv:1311.0283
46. J.M. Campbell, R.K. Ellis, MCFM for the Tevatron and the LHC. Nucl. Phys. B Proc. Suppl. **205–206**, 10 (2010). https://doi.org/10.1016/j.nuclphysbps.2010.08.011. arXiv:1007.3492
47. GEANT4 Collaboration, GEANT4—a simulation toolkit. Nucl. Instrum. Meth. A **506** 250, (2003). https://doi.org/10.1016/S0168-9002(03)01368-8
48. J. Allison et al., GEANT4 developments and applications. IEEE Trans. Nucl. Sci. **53**, 270 (2006). https://doi.org/10.1109/TNS.2006.869826
49. NNPDF Collaboration, Parton distributions with LHC data. Nucl. Phys. B **867** 244, (2013). https://doi.org/10.1016/j.nuclphysb.2012.10.003. arXiv:1207.1303
50. CMS Collaboration, The CMS trigger system. JINST **12** P01020, (2017). https://doi.org/10.1088/1748-0221/12/01/P01020. arXiv:1609.02366
51. M. Cacciari, G.P. Salam, G. Soyez, The anti-k_t jet clustering algorithm. JHEP **04**, 063 (2008). https://doi.org/10.1088/1126-6708/2008/04/063. arXiv:0802.1189
52. M. Cacciari, G.P. Salam, G. Soyez, FastJet user manual. Eur. Phys. J. C **72**, 1896 (2012). https://doi.org/10.1140/epjc/s10052-012-1896-2. arXiv:1111.6097
53. Particle Data Group, C. Patrignani et al., Review of particle physics. Chin. Phys. C **40** 100001 (2016). https://doi.org/10.1088/1674-1137/40/10/100001
54. M. Cacciari, G.P. Salam, Dispelling the N^3 myth for the k_t jet-finder. Phys. Lett. B **641**, 57 (2006). https://doi.org/10.1016/j.physletb.2006.08.037. arXiv:hep-ph/0512210
55. CMS Collaboration, Determination of jet energy calibration and transverse momentum resolution in CMS. JINST **6** P11002 (2011). https://doi.org/10.1088/1748-0221/6/11/P11002. arXiv:1107.4277
56. CMS Collaboration, Jet algorithms performance in 13 TeV data. CMS Physics Analysis Summary CMS-PAS-JME-16-003 (2017)
57. CMS Collaboration, Pileup jet identification. CMS Physics Analysis Summary (2013)
58. CMS Collaboration, Performance of quark/gluon discrimination using pp collision data at $\sqrt{s} = 8$ TeV. CMS Physics Analysis Summary CMS-PAS-JME-13-002 (2013)
59. H. Voss, A. Höcker, J. Stelzer, F. Tegenfeldt, TMVA, the toolkit for multivariate data analysis with ROOT, in *XIth International Workshop on Advanced Computing and Analysis Techniques in Physics Research (ACAT)*, p. 40. (2007). arXiv:physics/0703039
60. G. Cowan, K. Cranmer, E. Gross, O. Vitells, Asymptotic formulae for likelihood-based tests of new physics. Eur. Phys. J. C **71**, 1554 (2011). https://doi.org/10.1140/epjc/s10052-011-1554-0. arXiv:1007.1727. [Erratum: 10.1140/epjc/s10052-013-2501-z]
61. CMS Collaboration, CMS luminosity measurements for the 2016 data taking period. CMS Physics Analysis Summary CMS-PAS-LUM-17-001 (2017)
62. CMS Collaboration, Measurements of inclusive W and Z cross sections in pp collisions at $\sqrt{s} = 7$ TeV. JHEP **01** 080, (2011). https://doi.org/10.1007/JHEP01(2011)080. arXiv:1012.2466
63. C. Degrande et al., Studies of vector boson scattering and triboson production with DELPHES parametrized fast simulation for Snowmass 2013. (2013). arXiv:1309.7452
64. Particle Data Group, Review of particle physics. J. Phys. G **37** 075021 (2010). https://doi.org/10.1088/0954-3899/37/7A/075021
65. The LEP Electroweak Working Group, Electroweak measurements in electron-positron collisions at W-boson-pair energies at LEP. Phys. Rept. **532** 119 (2013). https://doi.org/10.1016/j.physrep.2013.07.004. arXiv:1302.3415
66. ATLAS Collaboration, Measurement of WW/WZ $\to \ell\nu$qq$'$ production with the hadronically decaying boson reconstructed as one or two jets in pp collisions at $\sqrt{s} = 8$ TeV with ATLAS, and constraints on anomalous gauge couplings. Eur. Phys. J. C **77** 563 (2017). https://doi.org/10.1140/epjc/s10052-017-5084-2. arXiv:1706.01702

67. ATLAS Collaboration, Measurements of $W^{\pm}Z$ production cross sections in pp collisions at $\sqrt{s} = 8$ TeV with the ATLAS detector and limits on anomalous gauge boson self-couplings. Phys. Rev. D **93** 092004 (2016). https://doi.org/10.1103/PhysRevD.93.092004. arXiv:1603.02151
68. CMS Collaboration, Search for anomalous couplings in boosted WW/WZ $\rightarrow \ell\nu q\bar{q}$ production in proton-proton collisions at $\sqrt{s} = 8$ TeV. Phys. Lett. B **772** 21 (2017). https://doi.org/10.1016/j.physletb.2017.06.009. arXiv:1703.06095
69. CMS Collaboration, Measurement of the WZ production cross section in pp collisions at $\sqrt{s} = 7$ and 8 TeV and search for anomalous triple gauge couplings at $\sqrt{s} = 8$ TeV. Eur. Phys. J. C **77** 236 (2017). https://doi.org/10.1140/epjc/s10052-017-4730-z. arXiv:1609.05721
70. K. Hagiwara, R.D. Peccei, D. Zeppenfeld, Probing the weak boson sector in $e^+e^- \rightarrow W^+W^-$. Nucl. Phys. B **282**, 253 (1987). https://doi.org/10.1016/0550-3213(87)90685-7
71. CMS Collaboration, Tracking and primary vertex results in first 7 TeV collisions. CMS Physics Analysis Summary CMS-PAS-TRK-10-005, (2010)
72. CMS Collaboration, Commissioning of trackjets in pp collisions at $\sqrt{s} = 7$ TeV., CMS Physics Analysis Summary CMS-PAS-JME-10-006 (2010)
73. CMS Collaboration, Performance of jet reconstruction with charged tracks only. CMS Physics Analysis Summary CMS-PAS-JME-08-001 (2009)

CMS Collaboration

Yerevan Physics Institute, Yerevan, Armenia
A. M. Sirunyan, A. Tumasyan

Institut für Hochenergiephysik, Wien, Austria
W. Adam, F. Ambrogi, E. Asilar, T. Bergauer, J. Brandstetter, E. Brondolin, M. Dragicevic, J. Erö, A. Escalante Del Valle, M. Flechl, M. Friedl, R. Frühwirth[1], V. M. Ghete, J. Grossmann, J. Hrubec, M. Jeitler[1], A. König, N. Krammer, I. Krätschmer, D. Liko, T. Madlener, I. Mikulec, E. Pree, N. Rad, H. Rohringer, J. Schieck[1], R. Schöfbeck, M. Spanring, D. Spitzbart, A. Taurok, W. Waltenberger, J. Wittmann, C.-E. Wulz[1], M. Zarucki

Institute for Nuclear Problems, Minsk, Belarus
V. Chekhovsky, V. Mossolov, J. Suarez Gonzalez

Universiteit Antwerpen, Antwerpen, Belgium
E. A. De Wolf, D. Di Croce, X. Janssen, J. Lauwers, M. Pieters, M. Van De Klundert, H. Van Haevermaet, P. Van Mechelen, N. Van Remortel

Vrije Universiteit Brussel, Brussel, Belgium
S. Abu Zeid, F. Blekman, J. D'Hondt, I. De Bruyn, J. De Clercq, K. Deroover, G. Flouris, D. Lontkovskyi, S. Lowette, I. Marchesini, S. Moortgat, L. Moreels, Q. Python, K. Skovpen, S. Tavernier, W. Van Doninck, P. Van Mulders, I. Van Parijs

Université Libre de Bruxelles, Bruxelles, Belgium
D. Beghin, B. Bilin, H. Brun, B. Clerbaux, G. De Lentdecker, H. Delannoy, B. Dorney, G. Fasanella, L. Favart, R. Goldouzian, A. Grebenyuk, A. K. Kalsi, T. Lenzi, J. Luetic, T. Maerschalk, T. Seva, E. Starling, C. Vander Velde, P. Vanlaer, D. Vannerom, R. Yonamine, F. Zenoni

Ghent University, Ghent, Belgium
T. Cornelis, D. Dobur, A. Fagot, M. Gul, I. Khvastunov[2], D. Poyraz, C. Roskas, D. Trocino, M. Tytgat, W. Verbeke, M. Vit, N. Zaganidis

Université Catholique de Louvain, Louvain-la-Neuve, Belgium
H. Bakhshiansohi, O. Bondu, S. Brochet, G. Bruno, C. Caputo, A. Caudron, P. David, S. De Visscher, C. Delaere, M. Delcourt, B. Francois, A. Giammanco, G. Krintiras, V. Lemaitre, A. Magitteri, A. Mertens, M. Musich, K. Piotrzkowski, L. Quertenmont, A. Saggio, M. Vidal Marono, S. Wertz, J. Zobec

Centro Brasileiro de Pesquisas Fisicas, Rio de Janeiro, Brazil
W. L. Aldá Júnior, F. L. Alves, G. A. Alves, L. Brito, G. Correia Silva, C. Hensel, A. Moraes, M. E. Pol, P. Rebello Teles

Universidade do Estado do Rio de Janeiro, Rio de Janeiro, Brazil
E. Belchior Batista Das Chagas, W. Carvalho, J. Chinellato[3], E. Coelho, E. M. Da Costa, G. G. Da Silveira[4], D. De Jesus Damiao, S. Fonseca De Souza, L. M. Huertas Guativa, H. Malbouisson, M. Melo De Almeida, C. Mora Herrera, L. Mundim, H. Nogima, L. J. Sanchez Rosas, A. Santoro, A. Sznajder, M. Thiel, E. J. Tonelli Manganote[3], F. Torres Da Silva De Araujo, A. Vilela Pereira

Universidade Estadual Paulista [a], Universidade Federal do ABC [b], São Paulo, Brazil
S. Ahuja[a], C. A. Bernardes[a], T. R. Fernandez Perez Tomei[a], E. M. Gregores[b], P. G. Mercadante[b], S. F. Novaes[a], Sandra S. Padula[a], D. Romero Abad[b], J. C. Ruiz Vargas[a]

Institute for Nuclear Research and Nuclear Energy, Bulgarian Academy of Sciences, Sofia, Bulgaria
A. Aleksandrov, R. Hadjiiska, P. Iaydjiev, A. Marinov, M. Misheva, M. Rodozov, M. Shopova, G. Sultanov

University of Sofia, Sofia, Bulgaria
A. Dimitrov, L. Litov, B. Pavlov, P. Petkov

Beihang University, Beijing, China
W. Fang[5], X. Gao[5], L. Yuan

Institute of High Energy Physics, Beijing, China
M. Ahmad, J. G. Bian, G. M. Chen, H. S. Chen, M. Chen, Y. Chen, C. H. Jiang, D. Leggat, H. Liao, Z. Liu, F. Romeo, S. M. Shaheen, A. Spiezia, J. Tao, C. Wang, Z. Wang, E. Yazgan, H. Zhang, J. Zhao

State Key Laboratory of Nuclear Physics and Technology, Peking University, Beijing, China
Y. Ban, G. Chen, J. Li, Q. Li, S. Liu, Y. Mao, S. J. Qian, D. Wang, Z. Xu

Tsinghua University, Beijing, China
Y. Wang

Universidad de Los Andes, Bogota, Colombia
C. Avila, A. Cabrera, C. A. Carrillo Montoya, L. F. Chaparro Sierra, C. Florez, C. F. González Hernández, J. D. Ruiz Alvarez, M. A. Segura Delgado

Faculty of Electrical Engineering, Mechanical Engineering and Naval Architecture, University of Split, Split, Croatia
B. Courbon, N. Godinovic, D. Lelas, I. Puljak, P. M. Ribeiro Cipriano, T. Sculac

University of Split, Faculty of Science, Split, Croatia
Z. Antunovic, M. Kovac

Institute Rudjer Boskovic, Zagreb, Croatia
V. Brigljevic, D. Ferencek, K. Kadija, B. Mesic, A. Starodumov[6], T. Susa

University of Cyprus, Nicosia, Cyprus
M. W. Ather, A. Attikis, G. Mavromanolakis, J. Mousa, C. Nicolaou, F. Ptochos, P. A. Razis, H. Rykaczewski

Charles University, Prague, Czech Republic
M. Finger[7], M. Finger Jr.[7]

Universidad San Francisco de Quito, Quito, Ecuador
E. Carrera Jarrin

Academy of Scientific Research and Technology of the Arab Republic of Egypt, Egyptian Network of High Energy Physics, Cairo, Egypt
E. El-khateeb[8], A. Ellithi Kamel[9], M. A. Mahmoud[10,11]

National Institute of Chemical Physics and Biophysics, Tallinn, Estonia
S. Bhowmik, R. K. Dewanjee, M. Kadastik, L. Perrini, M. Raidal, C. Veelken

Department of Physics, University of Helsinki, Helsinki, Finland
P. Eerola, H. Kirschenmann, J. Pekkanen, M. Voutilainen

Helsinki Institute of Physics, Helsinki, Finland
J. Havukainen, J. K. Heikkilä, T. Järvinen, V. Karimäki, R. Kinnunen, T. Lampén, K. Lassila-Perini, S. Laurila, S. Lehti, T. Lindén, P. Luukka, T. Mäenpää, H. Siikonen, E. Tuominen, J. Tuominiemi

Lappeenranta University of Technology, Lappeenranta, Finland
T. Tuuva

IRFU, CEA, Université Paris-Saclay, Gif-sur-Yvette, France
M. Besancon, F. Couderc, M. Dejardin, D. Denegri, J. L. Faure, F. Ferri, S. Ganjour, S. Ghosh, A. Givernaud, P. Gras, G. Hamel de Monchenault, P. Jarry, C. Leloup, E. Locci, M. Machet, J. Malcles, G. Negro, J. Rander, A. Rosowsky, M. Ö. Sahin, M. Titov

Laboratoire Leprince-Ringuet, Ecole polytechnique, CNRS/IN2P3, Université Paris-Saclay, Palaiseau, France
A. Abdulsalam[12], C. Amendola, I. Antropov, S. Baffioni, F. Beaudette, P. Busson, L. Cadamuro, C. Charlot, R. Granier de Cassagnac, M. Jo, I. Kucher, S. Lisniak, A. Lobanov, J. Martin Blanco, M. Nguyen, C. Ochando, G. Ortona, P. Paganini, P. Pigard, R. Salerno, J. B. Sauvan, Y. Sirois, A. G. Stahl Leiton, Y. Yilmaz, A. Zabi, A. Zghiche

Université de Strasbourg, CNRS, IPHC UMR 7178, 67000 Strasbourg, France
J.-L. Agram[13], J. Andrea, D. Bloch, J.-M. Brom, M. Buttignol, E. C. Chabert, C. Collard, E. Conte[13], X. Coubez, F. Drouhin[13], J.-C. Fontaine[13], D. Gelé, U. Goerlach, M. Jansová, P. Juillot, A.-C. Le Bihan, N. Tonon, P. Van Hove

Centre de Calcul de l'Institut National de Physique Nucleaire et de Physique des Particules, CNRS/IN2P3, Villeurbanne, France
S. Gadrat

Université de Lyon, Université Claude Bernard Lyon 1, CNRS-IN2P3, Institut de Physique Nucléaire de Lyon, Villeurbanne, France
S. Beauceron, C. Bernet, G. Boudoul, N. Chanon, R. Chierici, D. Contardo, P. Depasse, H. El Mamouni, J. Fay, L. Finco, S. Gascon, M. Gouzevitch, G. Grenier, B. Ille, F. Lagarde, I. B. Laktineh, H. Lattaud, M. Lethuillier, L. Mirabito, A. L. Pequegnot, S. Perries, A. Popov[14], V. Sordini, M. Vander Donckt, S. Viret, S. Zhang

Georgian Technical University, Tbilisi, Georgia
A. Khvedelidze[7]

Tbilisi State University, Tbilisi, Georgia
I. Bagaturia[15]

RWTH Aachen University, I. Physikalisches Institut, Aachen, Germany
C. Autermann, L. Feld, M. K. Kiesel, K. Klein, M. Lipinski, M. Preuten, C. Schomakers, J. Schulz, M. Teroerde, B. Wittmer, V. Zhukov[14]

RWTH Aachen University, III. Physikalisches Institut A, Aachen, Germany
A. Albert, D. Duchardt, M. Endres, M. Erdmann, S. Erdweg, T. Esch, R. Fischer, A. Güth, T. Hebbeker, C. Heidemann, K. Hoepfner, S. Knutzen, M. Merschmeyer, A. Meyer, P. Millet, S. Mukherjee, T. Pook, M. Radziej, H. Reithler, M. Rieger, F. Scheuch, D. Teyssier, S. Thüer

RWTH Aachen University, III. Physikalisches Institut B, Aachen, Germany
G. Flügge, B. Kargoll, T. Kress, A. Künsken, T. Müller, A. Nehrkorn, A. Nowack, C. Pistone, O. Pooth, A. Stahl[16]

Deutsches Elektronen-Synchrotron, Hamburg, Germany
M. Aldaya Martin, T. Arndt, C. Asawatangtrakuldee, K. Beernaert, O. Behnke, U. Behrens, A. Bermúdez Martínez, A. A. Bin Anuar, K. Borras[17], V. Botta, A. Campbell, P. Connor, C. Contreras-Campana, F. Costanza, A. De Wit, C. Diez Pardos, G. Eckerlin, D. Eckstein, T. Eichhorn, E. Eren, E. Gallo[18], J. Garay Garcia, A. Geiser, J. M. Grados Luyando, A. Grohsjean, P. Gunnellini, M. Guthoff, A. Harb, J. Hauk, M. Hempel[19], H. Jung, M. Kasemann, J. Keaveney, C. Kleinwort, I. Korol, D. Krücker, W. Lange, A. Lelek, T. Lenz, K. Lipka, W. Lohmann[19], R. Mankel, I.-A. Melzer-Pellmann, A. B. Meyer, M. Meyer, M. Missiroli, G. Mittag, J. Mnich, A. Mussgiller, D. Pitzl, A. Raspereza, M. Savitskyi, P. Saxena, R. Shevchenko, N. Stefaniuk, H. Tholen, G. P. Van Onsem, R. Walsh, Y. Wen, K. Wichmann, C. Wissing, O. Zenaiev

University of Hamburg, Hamburg, Germany
R. Aggleton, S. Bein, V. Blobel, M. Centis Vignali, T. Dreyer, E. Garutti, D. Gonzalez, J. Haller, A. Hinzmann, M. Hoffmann, A. Karavdina, G. Kasieczka, R. Klanner, R. Kogler, N. Kovalchuk, S. Kurz, D. Marconi, J. Multhaup, M. Niedziela, D. Nowatschin, T. Peiffer, A. Perieanu, A. Reimers, C. Scharf, P. Schleper, A. Schmidt, S. Schumann,

J. Schwandt, J. Sonneveld, H. Stadie, G. Steinbrück, F. M. Stober, M. Stöver, D. Troendle, E. Usai, A. Vanhoefer, B. Vormwald

Institut für Experimentelle Kernphysik, Karlsruhe, Germany
M. Akbiyik, C. Barth, M. Baselga, S. Baur, E. Butz, R. Caspart, T. Chwalek, F. Colombo, W. De Boer, A. Dierlamm, N. Faltermann, B. Freund, R. Friese, M. Giffels, M. A. Harrendorf, F. Hartmann[16], S. M. Heindl, U. Husemann, F. Kassel[16], S. Kudella, H. Mildner, M. U. Mozer, Th. Müller, M. Plagge, G. Quast, K. Rabbertz, M. Schröder, I. Shvetsov, G. Sieber, H. J. Simonis, R. Ulrich, S. Wayand, M. Weber, T. Weiler, S. Williamson, C. Wöhrmann, R. Wolf

Institute of Nuclear and Particle Physics (INPP), NCSR Demokritos, Aghia Paraskevi, Greece
G. Anagnostou, G. Daskalakis, T. Geralis, A. Kyriakis, D. Loukas, I. Topsis-Giotis

National and Kapodistrian University of Athens, Athens, Greece
G. Karathanasis, S. Kesisoglou, A. Panagiotou, N. Saoulidou, E. Tziaferi

National Technical University of Athens, Athens, Greece
K. Kousouris, I. Papakrivopoulos

University of Ioánnina, Ioannina, Greece
I. Evangelou, C. Foudas, P. Gianneios, P. Katsoulis, P. Kokkas, S. Mallios, N. Manthos, I. Papadopoulos, E. Paradas, J. Strologas, F. A. Triantis, D. Tsitsonis

MTA-ELTE Lendület CMS Particle and Nuclear Physics Group, Eötvös Loránd University, Budapest, Hungary
M. Csanad, N. Filipovic, G. Pasztor, O. Surányi, G. I. Veres[20]

Wigner Research Centre for Physics, Budapest, Hungary
G. Bencze, C. Hajdu, D. Horvath[21], Á. Hunyadi, F. Sikler, T. Á. Vámi, V. Veszpremi, G. Vesztergombi[20]

Institute of Nuclear Research ATOMKI, Debrecen, Hungary
N. Beni, S. Czellar, J. Karancsi[22], A. Makovec, J. Molnar, Z. Szillasi

Institute of Physics, University of Debrecen, Debrecen, Hungary
M. Bartók[20], P. Raics, Z. L. Trocsanyi, B. Ujvari

Indian Institute of Science (IISc), Bangalore, India
S. Choudhury, J. R. Komaragiri

National Institute of Science Education and Research, Bhubaneswar, India
S. Bahinipati[23], P. Mal, K. Mandal, A. Nayak[24], D. K. Sahoo[23], N. Sahoo, S. K. Swain

Panjab University, Chandigarh, India
S. Bansal, S. B. Beri, V. Bhatnagar, R. Chawla, N. Dhingra, R. Gupta, A. Kaur, M. Kaur, S. Kaur, R. Kumar, P. Kumari, A. Mehta, S. Sharma, J. B. Singh, G. Walia

University of Delhi, Delhi, India
A. Bhardwaj, S. Chauhan, B. C. Choudhary, R. B. Garg, S. Keshri, A. Kumar, Ashok Kumar, S. Malhotra, M. Naimuddin, K. Ranjan, Aashaq Shah, R. Sharma

Saha Institute of Nuclear Physics, HBNI, Kolkata, India
R. Bhardwaj[25], R. Bhattacharya, S. Bhattacharya, U. Bhawandeep[25], D. Bhowmik, S. Dey, S. Dutt[25], S. Dutta, S. Ghosh, N. Majumdar, A. Modak, K. Mondal, S. Mukhopadhyay, S. Nandan, A. Purohit, P. K. Rout, A. Roy, S. Roy Chowdhury, S. Sarkar, M. Sharan, B. Singh, S. Thakur[25]

Indian Institute of Technology Madras, Madras, India
P. K. Behera

Bhabha Atomic Research Centre, Mumbai, India
R. Chudasama, D. Dutta, V. Jha, V. Kumar, A. K. Mohanty[16], P. K. Netrakanti, L. M. Pant, P. Shukla, A. Topkar

Tata Institute of Fundamental Research-A, Mumbai, India
T. Aziz, S. Dugad, B. Mahakud, S. Mitra, G. B. Mohanty, N. Sur, B. Sutar

Tata Institute of Fundamental Research-B, Mumbai, India
S. Banerjee, S. Bhattacharya, S. Chatterjee, P. Das, M. Guchait, Sa. Jain, S. Kumar, M. Maity[26], G. Majumder, K. Mazumdar, T. Sarkar[26], N. Wickramage[27]

Indian Institute of Science Education and Research (IISER), Pune, India
S. Chauhan, S. Dube, V. Hegde, A. Kapoor, K. Kothekar, S. Pandey, A. Rane, S. Sharma

Institute for Research in Fundamental Sciences (IPM), Tehran, Iran
S. Chenarani[28], E. Eskandari Tadavani, S. M. Etesami[28], M. Khakzad, M. Mohammadi Najafabadi, M. Naseri, S. Paktinat Mehdiabadi[29], F. Rezaei Hosseinabadi, B. Safarzadeh[30], M. Zeinali

University College Dublin, Dublin, Ireland
M. Felcini, M. Grunewald

INFN Sezione di Bari [a], Università di Bari [b], Politecnico di Bari [c], Bari, Italy
M. Abbrescia[a,b], C. Calabria[a,b], A. Colaleo[a], D. Creanza[a,c], L. Cristella[a,b], N. De Filippis[a,c], M. De Palma[a,b], A. Di Florio[a,b], F. Errico[a,b], L. Fiore[a], G. Iaselli[a,c], S. Lezki[a,b], G. Maggi[a,c], B. Marangelli[a,b], M. Maggi[a], G. Miniello[a,b], S. My[a,b], S. Nuzzo[a,b], A. Pompili[a,b], G. Pugliese[a,c], R. Radogna[a], A. Ranieri[a], G. Selvaggi[a,b], A. Sharma[a], L. Silvestris[a,16], R. Venditti[a], P. Verwilligen[a], G. Zito[a]

INFN Sezione di Bologna [a], Università di Bologna [b], Bologna, Italy
G. Abbiendi[a], C. Battilana[a,b], D. Bonacorsi[a,b], L. Borgonovi[a,b], S. Braibant-Giacomelli[a,b], R. Campanini[a,b], P. Capiluppi[a,b], A. Castro[a,b], F. R. Cavallo[a], S. S. Chhibra[a,b], G. Codispoti[a,b], M. Cuffiani[a,b], G. M. Dallavalle[a], F. Fabbri[a], A. Fanfani[a,b], D. Fasanella[a,b], P. Giacomelli[a], C. Grandi[a], L. Guiducci[a,b], F. Iemmi, S. Marcellini[a], G. Masetti[a], A. Montanari[a], F. L. Navarria[a,b], A. Perrotta[a], A. M. Rossi[a,b], T. Rovelli[a,b], G. P. Siroli[a,b], N. Tosi[a]

INFN Sezione di Catania [a], Università di Catania [b], Catania, Italy
S. Albergo[a,b], S. Costa[a,b], A. Di Mattia[a], F. Giordano[a,b], R. Potenza[a,b], A. Tricomi[a,b], C. Tuve[a,b]

INFN Sezione di Firenze [a], Università di Firenze [b], Firenze, Italy
G. Barbagli[a], K. Chatterjee[a,b], V. Ciulli[a,b], C. Civinini[a], R. D'Alessandro[a,b], E. Focardi[a,b], G. Latino, P. Lenzi[a,b], M. Meschini[a], S. Paoletti[a], L. Russo[a,31], G. Sguazzoni[a], D. Strom[a], L. Viliani[a]

INFN Laboratori Nazionali di Frascati, Frascati, Italy
L. Benussi, S. Bianco, F. Fabbri, D. Piccolo, F. Primavera[16]

INFN Sezione di Genova [a], Università di Genova [b], Genova, Italy
V. Calvelli[a,b], F. Ferro[a], F. Ravera[a,b], E. Robutti[a], S. Tosi[a,b]

INFN Sezione di Milano-Bicocca [a], Università di Milano-Bicocca [b], Milan, Italy
A. Benaglia[a], A. Beschi[b], L. Brianza[a,b], F. Brivio[a,b], V. Ciriolo[a,b,16], M. E. Dinardo[a,b], S. Fiorendi[a,b], S. Gennai[a], A. Ghezzi[a,b], P. Govoni[a,b], M. Malberti[a,b], S. Malvezzi[a], R. A. Manzoni[a,b], D. Menasce[a], L. Moroni[a], M. Paganoni[a,b], K. Pauwels[a,b], D. Pedrini[a], S. Pigazzini[a,b,32], S. Ragazzi[a,b], T. Tabarelli de Fatis[a,b]

INFN Sezione di Napoli [a], Università di Napoli 'Federico II' [b], Napoli, Italy, Università della Basilicata [c], Potenza, Italy, Università G. Marconi [d], Roma, Italy
S. Buontempo[a], N. Cavallo[a,c], S. Di Guida[a,d,16], F. Fabozzi[a,c], F. Fienga[a,b], A. O. M. Iorio[a,b], W. A. Khan[a], L. Lista[a], S. Meola[a,d,16], P. Paolucci[a,16], C. Sciacca[a,b], F. Thyssen[a]

INFN Sezione di Padova [a], Università di Padova [b], Padova, Italy, Università di Trento [c], Trento, Italy
P. Azzi[a], N. Bacchetta[a], L. Benato[a,b], D. Bisello[a,b], A. Boletti[a,b], R. Carlin[a,b], A. Carvalho Antunes De Oliveira[a,b], P. Checchia[a], M. Dall'Osso[a,b], P. De Castro Manzano[a], U. Dosselli[a], F. Gasparini[a,b], U. Gasparini[a,b], A. Gozzelino[a], S. Lacaprara[a], P. Lujan, M. Margoni[a,b], A. T. Meneguzzo[a,b], N. Pozzobon[a,b], P. Ronchese[a,b], R. Rossin[a,b], F. Simonetto[a,b], A. Tiko, E. Torassa[a], M. Zanetti[a,b], P. Zotto[a,b], G. Zumerle[a,b]

INFN Sezione di Pavia [a], Università di Pavia [b], Pavia, Italy
A. Braghieri[a], A. Magnani[a], P. Montagna[a,b], S. P. Ratti[a,b], V. Re[a], M. Ressegotti[a,b], C. Riccardi[a,b], P. Salvini[a], I. Vai[a,b], P. Vitulo[a,b]

INFN Sezione di Perugia [a], Università di Perugia [b], Perugia, Italy
L. Alunni Solestizi[a,b], M. Biasini[a,b], G. M. Bilei[a], C. Cecchi[a,b], D. Ciangottini[a,b], L. Fanò[a,b], P. Lariccia[a,b], R. Leonardi[a,b], E. Manoni[a], G. Mantovani[a,b], V. Mariani[a,b], M. Menichelli[a], A. Rossi[a,b], A. Santocchia[a,b], D. Spiga[a]

INFN Sezione di Pisa [a], Università di Pisa [b], Scuola Normale Superiore di Pisa [c], Pisa, Italy
K. Androsov[a], P. Azzurri[a,16], G. Bagliesi[a], L. Bianchini[a], T. Boccali[a], L. Borrello, R. Castaldi[a], M. A. Ciocci[a,b], R. Dell'Orso[a], G. Fedi[a], L. Giannini[a,c], A. Giassi[a], M. T. Grippo[a,31], F. Ligabue[a,c], T. Lomtadze[a], E. Manca[a,c], G. Mandorli[a,c], A. Messineo[a,b], F. Palla[a], A. Rizzi[a,b], P. Spagnolo[a], R. Tenchini[a], G. Tonelli[a,b], A. Venturi[a], P. G. Verdini[a]

INFN Sezione di Roma [a], Sapienza Università di Roma [b], Rome, Italy
L. Barone[a,b], F. Cavallari[a], M. Cipriani[a,b], N. Daci[a], D. Del Re[a,b], E. Di Marco[a,b], M. Diemoz[a], S. Gelli[a,b], E. Longo[a,b], F. Margaroli[a,b], B. Marzocchi[a,b], P. Meridiani[a], G. Organtini[a,b], R. Paramatti[a,b], F. Preiato[a,b], S. Rahatlou[a,b], C. Rovelli[a], F. Santanastasio[a,b]

INFN Sezione di Torino [a], Università di Torino [b], Torino, Italy, Università del Piemonte Orientale [c], Novara, Italy
N. Amapane[a,b], R. Arcidiacono[a,c], S. Argiro[a,b], M. Arneodo[a,c], N. Bartosik[a], R. Bellan[a,b], C. Biino[a], N. Cartiglia[a], R. Castello[a,b], F. Cenna[a,b], M. Costa[a,b], R. Covarelli[a,b], A. Degano[a,b], N. Demaria[a], B. Kiani[a,b], C. Mariotti[a], S. Maselli[a], E. Migliore[a,b], V. Monaco[a,b], E. Monteil[a,b], M. Monteno[a], M. M. Obertino[a,b], L. Pacher[a,b], N. Pastrone[a], M. Pelliccioni[a], G. L. Pinna Angioni[a,b], A. Romero[a,b], M. Ruspa[a,c], R. Sacchi[a,b], K. Shchelina[a,b], V. Sola[a], A. Solano[a,b], A. Staiano[a], P. Traczyk[a,b]

INFN Sezione di Trieste [a], Università di Trieste [b], Trieste, Italy
S. Belforte[a], M. Casarsa[a], F. Cossutti[a], G. Della Ricca[a,b], A. Zanetti[a]

Kyungpook National University, Daegu, Korea
D. H. Kim, G. N. Kim, M. S. Kim, J. Lee, S. Lee, S. W. Lee, C. S. Moon, Y. D. Oh, S. Sekmen, D. C. Son, Y. C. Yang

Chonnam National University, Institute for Universe and Elementary Particles, Kwangju, Korea
H. Kim, D. H. Moon, G. Oh

Hanyang University, Seoul, Korea
J. A. Brochero Cifuentes, J. Goh, T. J. Kim

Korea University, Seoul, Korea
S. Cho, S. Choi, Y. Go, D. Gyun, S. Ha, B. Hong, Y. Jo, Y. Kim, K. Lee, K. S. Lee, S. Lee, J. Lim, S. K. Park, Y. Roh

Seoul National University, Seoul, Korea
J. Almond, J. Kim, J. S. Kim, H. Lee, K. Lee, K. Nam, S. B. Oh, B. C. Radburn-Smith, S. h. Seo, U. K. Yang, H. D. Yoo, G. B. Yu

University of Seoul, Seoul, Korea
H. Kim, J. H. Kim, J. S. H. Lee, I. C. Park

Sungkyunkwan University, Suwon, Korea
Y. Choi, C. Hwang, J. Lee, I. Yu

Vilnius University, Vilnius, Lithuania
V. Dudenas, A. Juodagalvis, J. Vaitkus

National Centre for Particle Physics, Universiti Malaya, Kuala Lumpur, Malaysia
I. Ahmed, Z. A. Ibrahim, M. A. B. Md Ali[33], F. Mohamad Idris[34], W. A. T. Wan Abdullah, M. N. Yusli, Z. Zolkapli

Centro de Investigacion y de Estudios Avanzados del IPN, Mexico City, Mexico
M. C. Duran-Osuna, H. Castilla-Valdez, E. De La Cruz-Burelo, G. Ramirez-Sanchez, I. Heredia-De La Cruz[35], R. I. Rabadan-Trejo, R. Lopez-Fernandez, J. Mejia Guisao, R Reyes-Almanza, A. Sanchez-Hernandez

Universidad Iberoamericana, Mexico City, Mexico
S. Carrillo Moreno, C. Oropeza Barrera, F. Vazquez Valencia

Benemerita Universidad Autonoma de Puebla, Puebla, Mexico
J. Eysermans, I. Pedraza, H. A. Salazar Ibarguen, C. Uribe Estrada

Universidad Autónoma de San Luis Potosí, San Luis Potosí, Mexico
A. Morelos Pineda

University of Auckland, Auckland, New Zealand
D. Krofcheck

University of Canterbury, Christchurch, New Zealand
P. H. Butler

National Centre for Physics, Quaid-I-Azam University, Islamabad, Pakistan
A. Ahmad, M. Ahmad, Q. Hassan, H. R. Hoorani, A. Saddique, M. A. Shah, M. Shoaib, M. Waqas

National Centre for Nuclear Research, Swierk, Poland
H. Bialkowska, M. Bluj, B. Boimska, T. Frueboes, M. Górski, M. Kazana, K. Nawrocki, M. Szleper, P. Zalewski

Institute of Experimental Physics, Faculty of Physics, University of Warsaw, Warsaw, Poland
K. Bunkowski, A. Byszuk[36], K. Doroba, A. Kalinowski, M. Konecki, J. Krolikowski, M. Misiura, M. Olszewski, A. Pyskir, M. Walczak

Laboratório de Instrumentação e Física Experimental de Partículas, Lisbon, Portugal
P. Bargassa, C. Beirão Da Cruz E Silva, A. Di Francesco, P. Faccioli, B. Galinhas, M. Gallinaro, J. Hollar, N. Leonardo, L. Lloret Iglesias, M. V. Nemallapudi, J. Seixas, G. Strong, O. Toldaiev, D. Vadruccio, J. Varela

Joint Institute for Nuclear Research, Dubna, Russia
S. Afanasiev, P. Bunin, M. Gavrilenko, I. Golutvin, I. Gorbunov, A. Kamenev, V. Karjavin, A. Lanev, A. Malakhov, V. Matveev[37,38], P. Moisenz, V. Palichik, V. Perelygin, S. Shmatov, S. Shulha, N. Skatchkov, V. Smirnov, N. Voytishin, A. Zarubin

Petersburg Nuclear Physics Institute, Gatchina (St. Petersburg), Russia
Y. Ivanov, V. Kim[39], E. Kuznetsova[40], P. Levchenko, V. Murzin, V. Oreshkin, I. Smirnov, D. Sosnov, V. Sulimov, L. Uvarov, S. Vavilov, A. Vorobyev

Institute for Nuclear Research, Moscow, Russia
Yu. Andreev, A. Dermenev, S. Gninenko, N. Golubev, A. Karneyeu, M. Kirsanov, N. Krasnikov, A. Pashenkov, D. Tlisov, A. Toropin

Institute for Theoretical and Experimental Physics, Moscow, Russia
V. Epshteyn, V. Gavrilov, N. Lychkovskaya, V. Popov, I. Pozdnyakov, G. Safronov, A. Spiridonov, A. Stepennov, V. Stolin, M. Toms, E. Vlasov, A. Zhokin

Moscow Institute of Physics and Technology, Moscow, Russia
T. Aushev, A. Bylinkin[38]

National Research Nuclear University 'Moscow Engineering Physics Institute' (MEPhI), Moscow, Russia
M. Chadeeva[41], P. Parygin, D. Philippov, S. Polikarpov, E. Popova, V. Rusinov

P.N. Lebedev Physical Institute, Moscow, Russia
V. Andreev, M. Azarkin[38], I. Dremin[38], M. Kirakosyan[38], S. V. Rusakov, A. Terkulov

Skobeltsyn Institute of Nuclear Physics; Lomonosov Moscow State University, Moscow, Russia
A. Baskakov, A. Belyaev, E. Boos, M. Dubinin[42], L. Dudko, A. Ershov, A. Gribushin, V. Klyukhin, O. Kodolova, I. Lokhtin, I. Miagkov, S. Obraztsov, S. Petrushanko, V. Savrin, A. Snigirev

Novosibirsk State University (NSU), Novosibirsk, Russia
V. Blinov[43], D. Shtol[43], Y. Skovpen[43]

State Research Center of Russian Federation, Institute for High Energy Physics of NRC & quot, Kurchatov Institute&quot, Protvino, Russia
I. Azhgirey, I. Bayshev, S. Bitioukov, D. Elumakhov, A. Godizov, V. Kachanov, A. Kalinin, D. Konstantinov, P. Mandrik, V. Petrov, R. Ryutin, A. Sobol, S. Troshin, N. Tyurin, A. Uzunian, A. Volkov

National Research Tomsk Polytechnic University, Tomsk, Russia
A. Babaev

Faculty of Physics and Vinca Institute of Nuclear Sciences, University of Belgrade, Belgrade, Serbia
P. Adzic[44], P. Cirkovic, D. Devetak, M. Dordevic, J. Milosevic

Centro de Investigaciones Energéticas Medioambientales y Tecnológicas (CIEMAT), Madrid, Spain
J. Alcaraz Maestre, A. Álvarez Fernández, I. Bachiller, M. Barrio Luna, M. Cerrada, N. Colino, B. De La Cruz, A. Delgado Peris, C. Fernandez Bedoya, J. P. Fernández Ramos, J. Flix, M. C. Fouz, O. Gonzalez Lopez, S. Goy Lopez, J. M. Hernandez, M. I. Josa, D. Moran, A. Pérez-Calero Yzquierdo, J. Puerta Pelayo, I. Redondo, L. Romero, M. S. Soares, A. Triossi

Universidad Autónoma de Madrid, Madrid, Spain
C. Albajar, J. F. de Trocóniz

Universidad de Oviedo, Oviedo, Spain
J. Cuevas, C. Erice, J. Fernandez Menendez, S. Folgueras, I. Gonzalez Caballero, J. R. González Fernández, E. Palencia Cortezon, S. Sanchez Cruz, P. Vischia, J. M. Vizan Garcia

Instituto de Física de Cantabria (IFCA), CSIC-Universidad de Cantabria, Santander, Spain
I. J. Cabrillo, A. Calderon, B. Chazin Quero, J. Duarte Campderros, M. Fernandez, P. J. Fernández Manteca, A. García Alonso, J. Garcia-Ferrero, G. Gomez, A. Lopez Virto, J. Marco, C. Martinez Rivero, P. Martinez Ruiz del Arbol, F. Matorras, J. Piedra Gomez, C. Prieels, T. Rodrigo, A. Ruiz-Jimeno, L. Scodellaro, N. Trevisani, I. Vila, R. Vilar Cortabitarte

CERN, European Organization for Nuclear Research, Geneva, Switzerland
D. Abbaneo, B. Akgun, E. Auffray, P. Baillon, A. H. Ball, D. Barney, J. Bendavid, M. Bianco, A. Bocci, C. Botta, T. Camporesi, M. Cepeda, G. Cerminara, E. Chapon, Y. Chen, D. d'Enterria, A. Dabrowski, V. Daponte, A. David, M. De Gruttola, A. De Roeck, N. Deelen, M. Dobson, T. du Pree, M. Dünser, N. Dupont, A. Elliott-Peisert, P. Everaerts, F. Fallavollita[45], G. Franzoni, J. Fulcher, W. Funk, D. Gigi, A. Gilbert, K. Gill, F. Glege, D. Gulhan, J. Hegeman, V. Innocente, A. Jafari, P. Janot, O. Karacheban[19], J. Kieseler, V. Knünz, A. Kornmayer, M. J. Kortelainen, M. Krammer[1], C. Lange, P. Lecoq, C. Lourenço, M. T. Lucchini, L. Malgeri, M. Mannelli, A. Martelli, F. Meijers, J. A. Merlin, S. Mersi, E. Meschi, P. Milenovic[46], F. Moortgat, M. Mulders, H. Neugebauer, J. Ngadiuba, S. Orfanelli, L. Orsini, F. Pantaleo[16], L. Pape, E. Perez, M. Peruzzi, A. Petrilli, G. Petrucciani, A. Pfeiffer, M. Pierini, F. M. Pitters, D. Rabady, A. Racz, T. Reis, G. Rolandi[47], M. Rovere, H. Sakulin, C. Schäfer, C. Schwick, M. Seidel, M. Selvaggi, A. Sharma, P. Silva, P. Sphicas[48], A. Stakia, J. Steggemann, M. Stoye, M. Tosi, D. Treille, A. Tsirou, V. Veckalns[49], M. Verweij, W. D. Zeuner

Paul Scherrer Institut, Villigen, Switzerland
W. Bertl†, L. Caminada[50], K. Deiters, W. Erdmann, R. Horisberger, Q. Ingram, H. C. Kaestli, D. Kotlinski, U. Langenegger, T. Rohe

Institute for Particle Physics and Astrophysics (IPA), ETH Zurich, Zurich, Switzerland
M. Backhaus, L. Bäni, P. Berger, B. Casal, N. Chernyavskaya, G. Dissertori, M. Dittmar, M. Donegà, C. Dorfer, C. Grab, C. Heidegger, D. Hits, J. Hoss, T. Klijnsma, W. Lustermann, B. Mangano, M. Marionneau, M. T. Meinhard, D. Meister, F. Micheli, P. Musella, F. Nessi-Tedaldi, F. Pandolfi, J. Pata, F. Pauss, G. Perrin, L. Perrozzi, M. Quittnat, M. Reichmann, D. A. Sanz Becerra, M. Schönenberger, L. Shchutska, V. R. Tavolaro, K. Theofilatos, M. L. Vesterbacka Olsson, R. Wallny, D. H. Zhu

Universität Zürich, Zurich, Switzerland
T. K. Aarrestad, C. Amsler[51], D. Brzhechko, M. F. Canelli, A. De Cosa, R. Del Burgo, S. Donato, C. Galloni, T. Hreus, B. Kilminster, I. Neutelings, D. Pinna, G. Rauco, P. Robmann, D. Salerno, K. Schweiger, C. Seitz, Y. Takahashi, A. Zucchetta

National Central University, Chung-Li, Taiwan
V. Candelise, Y. H. Chang, K. y. Cheng, T. H. Doan, Sh. Jain, R. Khurana, C. M. Kuo, W. Lin, A. Pozdnyakov, S. S. Yu

National Taiwan University (NTU), Taipei, Taiwan
P. Chang, Y. Chao, K. F. Chen, P. H. Chen, F. Fiori, W.-S. Hou, Y. Hsiung, Arun Kumar, Y. F. Liu, R.-S. Lu, E. Paganis, A. Psallidas, A. Steen, J. f. Tsai

Department of Physics, Faculty of Science, Chulalongkorn University, Bangkok, Thailand
B. Asavapibhop, K. Kovitanggoon, G. Singh, N. Srimanobhas

Physics Department, Science and Art Faculty, Çukurova University, Adana, Turkey
A. Bat, F. Boran, S. Cerci[52], S. Damarseckin, Z. S. Demiroglu, C. Dozen, I. Dumanoglu, S. Girgis, G. Gokbulut, Y. Guler, I. Hos[53], E. E. Kangal[54], O. Kara, A. Kayis Topaksu, U. Kiminsu, M. Oglakci, G. Onengut, K. Ozdemir[55], D. Sunar Cerci[52], B. Tali[52], U. G. Tok, S. Turkcapar, I. S. Zorbakir, C. Zorbilmez

Physics Department, Middle East Technical University, Ankara, Turkey
G. Karapinar[56], K. Ocalan[57], M. Yalvac, M. Zeyrek

Bogazici University, Istanbul, Turkey
E. Gülmez, M. Kaya[58], O. Kaya[59], S. Tekten, E. A. Yetkin[60]

Istanbul Technical University, Istanbul, Turkey
M. N. Agaras, S. Atay, A. Cakir, K. Cankocak, Y. Komurcu

Institute for Scintillation Materials of National Academy of Science of Ukraine, Kharkov, Ukraine
B. Grynyov

National Scientific Center, Kharkov Institute of Physics and Technology, Kharkov, Ukraine
L. Levchuk

University of Bristol, Bristol, United Kingdom
F. Ball, L. Beck, J. J. Brooke, D. Burns, E. Clement, D. Cussans, O. Davignon, H. Flacher, J. Goldstein, G. P. Heath, H. F. Heath, L. Kreczko, D. M. Newbold[61], S. Paramesvaran, T. Sakuma, S. Seif El Nasr-storey, D. Smith, V. J. Smith

Rutherford Appleton Laboratory, Didcot, United Kingdom
K. W. Bell, A. Belyaev[62], C. Brew, R. M. Brown, L. Calligaris, D. Cieri, D. J. A. Cockerill, J. A. Coughlan, K. Harder, S. Harper, J. Linacre, E. Olaiya, D. Petyt, C. H. Shepherd-Themistocleous, A. Thea, I. R. Tomalin, T. Williams, W. J. Womersley

Imperial College, London, United Kingdom
G. Auzinger, R. Bainbridge, P. Bloch, J. Borg, S. Breeze, O. Buchmuller, A. Bundock, S. Casasso, D. Colling, L. Corpe, P. Dauncey, G. Davies, M. Della Negra, R. Di Maria, Y. Haddad, G. Hall, G. Iles, T. James, M. Komm, R. Lane, C. Laner, L. Lyons, A.-M. Magnan, S. Malik, L. Mastrolorenzo, T. Matsushita, J. Nash[63], A. Nikitenko[6], V. Palladino, M. Pesaresi, A. Richards, A. Rose, E. Scott, C. Seez, A. Shtipliyski, T. Strebler, S. Summers, A. Tapper, K. Uchida, M. Vazquez Acosta[64], T. Virdee[16], N. Wardle, D. Winterbottom, J. Wright, S. C. Zenz

Brunel University, Uxbridge, United Kingdom
J. E. Cole, P. R. Hobson, A. Khan, P. Kyberd, A. Morton, I. D. Reid, L. Teodorescu, S. Zahid

Baylor University, Waco, USA
A. Borzou, K. Call, J. Dittmann, K. Hatakeyama, H. Liu, N. Pastika, C. Smith

Catholic University of America, Washington DC, USA
R. Bartek, A. Dominguez

The University of Alabama, Tuscaloosa, USA
A. Buccilli, S. I. Cooper, C. Henderson, P. Rumerio, C. West

Boston University, Boston, USA
D. Arcaro, A. Avetisyan, T. Bose, D. Gastler, D. Rankin, C. Richardson, J. Rohlf, L. Sulak, D. Zou

Brown University, Providence, USA
G. Benelli, D. Cutts, M. Hadley, J. Hakala, U. Heintz, J. M. Hogan[65], K. H. M. Kwok, E. Laird, G. Landsberg, J. Lee, Z. Mao, M. Narain, J. Pazzini, S. Piperov, S. Sagir, R. Syarif, D. Yu

University of California, Davis, Davis, USA
R. Band, C. Brainerd, R. Breedon, D. Burns, M. Calderon De LaBarca Sanchez, M. Chertok, J. Conway, R. Conway, P. T. Cox, R. Erbacher, C. Flores, G. Funk, W. Ko, R. Lander, C. Mclean, M. Mulhearn, D. Pellett, J. Pilot, S. Shalhout, M. Shi, J. Smith, D. Stolp, D. Taylor, K. Tos, M. Tripathi, Z. Wang, F. Zhang

University of California, Los Angeles, USA
M. Bachtis, C. Bravo, R. Cousins, A. Dasgupta, A. Florent, J. Hauser, M. Ignatenko, N. Mccoll, S. Regnard, D. Saltzberg, C. Schnaible, V. Valuev

University of California, Riverside, Riverside, USA
E. Bouvier, K. Burt, R. Clare, J. Ellison, J. W. Gary, S. M. A. Ghiasi Shirazi, G. Hanson, G. Karapostoli, E. Kennedy, F. Lacroix, O. R. Long, M. Olmedo Negrete, M. I. Paneva, W. Si, L. Wang, H. Wei, S. Wimpenny, B. R. Yates

University of California, San Diego, La Jolla, USA
J. G. Branson, S. Cittolin, M. Derdzinski, R. Gerosa, D. Gilbert, B. Hashemi, A. Holzner, D. Klein, G. Kole, V. Krutelyov, J. Letts, M. Masciovecchio, D. Olivito, S. Padhi, M. Pieri, M. Sani, V. Sharma, S. Simon, M. Tadel, A. Vartak, S. Wasserbaech[66], J. Wood, F. Würthwein, A. Yagil, G. Zevi Della Porta

Department of Physics, University of California, Santa Barbara, Santa Barbara, USA
N. Amin, R. Bhandari, J. Bradmiller-Feld, C. Campagnari, M. Citron, A. Dishaw, V. Dutta, M. Franco Sevilla, L. Gouskos, R. Heller, J. Incandela, A. Ovcharova, H. Qu, J. Richman, D. Stuart, I. Suarez, J. Yoo

California Institute of Technology, Pasadena, USA
D. Anderson, A. Bornheim, J. Bunn, J. M. Lawhorn, H. B. Newman, T. Q. Nguyen, C. Pena, M. Spiropulu, J. R. Vlimant, R. Wilkinson, S. Xie, Z. Zhang, R. Y. Zhu

Carnegie Mellon University, Pittsburgh, USA
M. B. Andrews, T. Ferguson, T. Mudholkar, M. Paulini, J. Russ, M. Sun, H. Vogel, I. Vorobiev, M. Weinberg

University of Colorado Boulder, Boulder, USA
J. P. Cumalat, W. T. Ford, F. Jensen, A. Johnson, M. Krohn, S. Leontsinis, E. Macdonald, T. Mulholland, K. Stenson, K. A. Ulmer, S. R. Wagner

Cornell University, Ithaca, USA
J. Alexander, J. Chaves, Y. Cheng, J. Chu, A. Datta, S. Dittmer, K. Mcdermott, N. Mirman, J. R. Patterson, D. Quach, A. Rinkevicius, A. Ryd, L. Skinnari, L. Soffi, S. M. Tan, Z. Tao, J. Thom, J. Tucker, P. Wittich, M. Zientek

Fermi National Accelerator Laboratory, Batavia, USA
S. Abdullin, M. Albrow, M. Alyari, G. Apollinari, A. Apresyan, A. Apyan, S. Banerjee, L. A. T. Bauerdick, A. Beretvas, J. Berryhill, P. C. Bhat, G. Bolla[†], K. Burkett, J. N. Butler, A. Canepa, G. B. Cerati, H. W. K. Cheung, F. Chlebana, M. Cremonesi, J. Duarte, V. D. Elvira, J. Freeman, Z. Gecse, E. Gottschalk, L. Gray, D. Green, S. Grünendahl, O. Gutsche, J. Hanlon, R. M. Harris, S. Hasegawa, J. Hirschauer, Z. Hu, B. Jayatilaka, S. Jindariani, M. Johnson, U. Joshi, B. Klima, B. Kreis, S. Lammel, D. Lincoln, R. Lipton, M. Liu, T. Liu, R. Lopes De Sá, J. Lykken, K. Maeshima, N. Magini, J. M. Marraffino, D. Mason, P. McBride, P. Merkel, S. Mrenna, S. Nahn, V. O'Dell, K. Pedro, O. Prokofyev, G. Rakness, L. Ristori, A. Savoy-Navarro[67], B. Schneider, E. Sexton-Kennedy, A. Soha, W. J. Spalding, L. Spiegel, S. Stoynev, J. Strait, N. Strobbe, L. Taylor, S. Tkaczyk, N. V. Tran, L. Uplegger, E. W. Vaandering, C. Vernieri, M. Verzocchi, R. Vidal, M. Wang, H. A. Weber, A. Whitbeck, W. Wu

University of Florida, Gainesville, USA
D. Acosta, P. Avery, P. Bortignon, D. Bourilkov, A. Brinkerhoff, A. Carnes, M. Carver, D. Curry, R. D. Field, I. K. Furic, S. V. Gleyzer, B. M. Joshi, J. Konigsberg, A. Korytov, K. Kotov, P. Ma, K. Matchev, H. Mei, G. Mitselmakher, K. Shi, D. Sperka, N. Terentyev, L. Thomas, J. Wang, S. Wang, J. Yelton

Florida International University, Miami, USA
Y. R. Joshi, S. Linn, P. Markowitz, J. L. Rodriguez

Florida State University, Tallahassee, USA
A. Ackert, T. Adams, A. Askew, S. Hagopian, V. Hagopian, K. F. Johnson, T. Kolberg, G. Martinez, T. Perry, H. Prosper, A. Saha, A. Santra, V. Sharma, R. Yohay

Florida Institute of Technology, Melbourne, USA
M. M. Baarmand, V. Bhopatkar, S. Colafranceschi, M. Hohlmann, D. Noonan, T. Roy, F. Yumiceva

University of Illinois at Chicago (UIC), Chicago, USA
M. R. Adams, L. Apanasevich, D. Berry, R. R. Betts, R. Cavanaugh, X. Chen, O. Evdokimov, C. E. Gerber, D. A. Hangal, D. J. Hofman, K. Jung, J. Kamin, I. D. Sandoval Gonzalez, M. B. Tonjes, N. Varelas, H. Wang, Z. Wu, J. Zhang

The University of Iowa, Iowa City, USA
B. Bilki[68], W. Clarida, K. Dilsiz[69], S. Durgut, R. P. Gandrajula, M. Haytmyradov, V. Khristenko, J.-P. Merlo, H. Mermerkaya[70], A. Mestvirishvili, A. Moeller, J. Nachtman, H. Ogul[71], Y. Onel, F. Ozok[72], A. Penzo, C. Snyder, E. Tiras, J. Wetzel, K. Yi

Johns Hopkins University, Baltimore, USA
B. Blumenfeld, A. Cocoros, N. Eminizer, D. Fehling, L. Feng, A. V. Gritsan, P. Maksimovic, J. Roskes, U. Sarica, M. Swartz, M. Xiao, C. You

The University of Kansas, Lawrence, USA
A. Al-bataineh, P. Baringer, A. Bean, S. Boren, J. Bowen, J. Castle, S. Khalil, A. Kropivnitskaya, D. Majumder, W. Mcbrayer, M. Murray, C. Rogan, C. Royon, S. Sanders, E. Schmitz, J. D. Tapia Takaki, Q. Wang

Kansas State University, Manhattan, USA
A. Ivanov, K. Kaadze, Y. Maravin, A. Mohammadi, L. K. Saini, N. Skhirtladze

Lawrence Livermore National Laboratory, Livermore, USA
F. Rebassoo, D. Wright

University of Maryland, College Park, USA
A. Baden, O. Baron, A. Belloni, S. C. Eno, Y. Feng, C. Ferraioli, N. J. Hadley, S. Jabeen, G. Y. Jeng, R. G. Kellogg, J. Kunkle, A. C. Mignerey, F. Ricci-Tam, Y. H. Shin, A. Skuja, S. C. Tonwar

Massachusetts Institute of Technology, Cambridge, USA
D. Abercrombie, B. Allen, V. Azzolini, R. Barbieri, A. Baty, G. Bauer, R. Bi, S. Brandt, W. Busza, I. A. Cali, M. D'Alfonso, Z. Demiragli, G. Gomez Ceballos, M. Goncharov, P. Harris, D. Hsu, M. Hu, Y. Iiyama, G. M. Innocenti, M. Klute, D. Kovalskyi, Y.-J. Lee, A. Levin, P. D. Luckey, B. Maier, A. C. Marini, C. Mcginn, C. Mironov, S. Narayanan, X. Niu, C. Paus, C. Roland, G. Roland, J. Salfeld-Nebgen, G. S. F. Stephans, K. Sumorok, K. Tatar, D. Velicanu, J. Wang, T. W. Wang, B. Wyslouch, S. Zhaozhong

University of Minnesota, Minneapolis, USA
A. C. Benvenuti, R. M. Chatterjee, A. Evans, P. Hansen, S. Kalafut, Y. Kubota, Z. Lesko, J. Mans, S. Nourbakhsh, N. Ruckstuhl, R. Rusack, J. Turkewitz, M. A. Wadud

University of Mississippi, Oxford, USA
J. G. Acosta, S. Oliveros

University of Nebraska-Lincoln, Lincoln, USA
E. Avdeeva, K. Bloom, D. R. Claes, C. Fangmeier, F. Golf, R. Gonzalez Suarez, R. Kamalieddin, I. Kravchenko, J. Monroy, J. E. Siado, G. R. Snow, B. Stieger

State University of New York at Buffalo, Buffalo, USA
J. Dolen, A. Godshalk, C. Harrington, I. Iashvili, D. Nguyen, A. Parker, S. Rappoccio, B. Roozbahani

Northeastern University, Boston, USA
G. Alverson, E. Barberis, C. Freer, A. Hortiangtham, A. Massironi, D. M. Morse, T. Orimoto, R. Teixeira De Lima, T. Wamorkar, B. Wang, A. Wisecarver, D. Wood

Northwestern University, Evanston, USA
S. Bhattacharya, O. Charaf, K. A. Hahn, N. Mucia, N. Odell, M. H. Schmitt, K. Sung, M. Trovato, M. Velasco

University of Notre Dame, Notre Dame, USA
R. Bucci, N. Dev, M. Hildreth, K. Hurtado Anampa, C. Jessop, D. J. Karmgard, N. Kellams, K. Lannon, W. Li, N. Loukas, N. Marinelli, F. Meng, C. Mueller, Y. Musienko[37], M. Planer, A. Reinsvold, R. Ruchti, P. Siddireddy, G. Smith, S. Taroni, M. Wayne, A. Wightman, M. Wolf, A. Woodard

The Ohio State University, Columbus, USA
J. Alimena, L. Antonelli, B. Bylsma, L. S. Durkin, S. Flowers, B. Francis, A. Hart, C. Hill, W. Ji, T. Y. Ling, W. Luo, B. L. Winer, H. W. Wulsin

Princeton University, Princeton, USA
S. Cooperstein, O. Driga, P. Elmer, J. Hardenbrook, P. Hebda, S. Higginbotham, A. Kalogeropoulos, D. Lange, J. Luo, D. Marlow, K. Mei, I. Ojalvo, J. Olsen, C. Palmer, P. Piroué, D. Stickland, C. Tully

University of Puerto Rico, Mayaguez, USA
S. Malik, S. Norberg

Purdue University, West Lafayette, USA
A. Barker, V. E. Barnes, S. Das, L. Gutay, M. Jones, A. W. Jung, A. Khatiwada, D. H. Miller, N. Neumeister, C. C. Peng, H. Qiu, J. F. Schulte, J. Sun, F. Wang, R. Xiao, W. Xie

Purdue University Northwest, Hammond, USA
T. Cheng, N. Parashar

Rice University, Houston, USA
Z. Chen, K. M. Ecklund, S. Freed, F. J. M. Geurts, M. Guilbaud, M. Kilpatrick, W. Li, B. Michlin, B. P. Padley, J. Roberts, J. Rorie, W. Shi, Z. Tu, J. Zabel, A. Zhang

University of Rochester, Rochester, USA
A. Bodek, P. de Barbaro, R. Demina, Y. t. Duh, T. Ferbel, M. Galanti, A. Garcia-Bellido, J. Han, O. Hindrichs, A. Khukhunaishvili, K. H. Lo, P. Tan, M. Verzetti

The Rockefeller University, New York, USA
R. Ciesielski, K. Goulianos, C. Mesropian

Rutgers, The State University of New Jersey, Piscataway, USA
A. Agapitos, J. P. Chou, Y. Gershtein, T. A. Gómez Espinosa, E. Halkiadakis, M. Heindl, E. Hughes, S. Kaplan, R. Kunnawalkam Elayavalli, S. Kyriacou, A. Lath, R. Montalvo, K. Nash, M. Osherson, H. Saka, S. Salur, S. Schnetzer, D. Sheffield, S. Somalwar, R. Stone, S. Thomas, P. Thomassen, M. Walker

University of Tennessee, Knoxville, USA
A. G. Delannoy, J. Heideman, G. Riley, K. Rose, S. Spanier, K. Thapa

Texas A & M University, College Station, USA
O. Bouhali[73], A. Castaneda Hernandez[73], A. Celik, M. Dalchenko, M. De Mattia, A. Delgado, S. Dildick, R. Eusebi, J. Gilmore, T. Huang, T. Kamon[74], R. Mueller, Y. Pakhotin, R. Patel, A. Perloff, L. Perniè, D. Rathjens, A. Safonov, A. Tatarinov

Texas Tech University, Lubbock, USA
N. Akchurin, J. Damgov, F. De Guio, P. R. Dudero, J. Faulkner, E. Gurpinar, S. Kunori, K. Lamichhane, S. W. Lee, T. Mengke, S. Muthumuni, T. Peltola, S. Undleeb, I. Volobouev, Z. Wang

Vanderbilt University, Nashville, USA
S. Greene, A. Gurrola, R. Janjam, W. Johns, C. Maguire, A. Melo, H. Ni, K. Padeken, P. Sheldon, S. Tuo, J. Velkovska, Q. Xu

University of Virginia, Charlottesville, USA
M. W. Arenton, P. Barria, B. Cox, R. Hirosky, M. Joyce, A. Ledovskoy, H. Li, C. Neu, T. Sinthuprasith, Y. Wang, E. Wolfe, F. Xia

Wayne State University, Detroit, USA
R. Harr, P. E. Karchin, N. Poudyal, J. Sturdy, P. Thapa, S. Zaleski

University of Wisconsin, Madison, Madison, WI, USA
M. Brodski, J. Buchanan, C. Caillol, D. Carlsmith, S. Dasu, L. Dodd, S. Duric, B. Gomber, M. Grothe, M. Herndon, A. Hervé, U. Hussain, P. Klabbers, A. Lanaro, A. Levine, K. Long, R. Loveless, V. Rekovic, T. Ruggles, A. Savin, N. Smith, W. H. Smith, N. Woods

† **Deceased**

1: Also at Vienna University of Technology, Vienna, Austria
2: Also at IRFU; CEA; Université Paris-Saclay, Gif-sur-Yvette, France
3: Also at Universidade Estadual de Campinas, Campinas, Brazil
4: Also at Federal University of Rio Grande do Sul, Porto Alegre, Brazil
5: Also at Université Libre de Bruxelles, Bruxelles, Belgium
6: Also at Institute for Theoretical and Experimental Physics, Moscow, Russia
7: Also at Joint Institute for Nuclear Research, Dubna, Russia
8: Now at Ain Shams University, Cairo, Egypt
9: Now at Cairo University, Cairo, Egypt
10: Also at Fayoum University, El-Fayoum, Egypt
11: Now at British University in Egypt, Cairo, Egypt
12: Also at Department of Physics; King Abdulaziz University, Jeddah, Saudi Arabia
13: Also at Université de Haute Alsace, Mulhouse, France
14: Also at Skobeltsyn Institute of Nuclear Physics, Lomonosov Moscow State University, Moscow, Russia
15: Also at Ilia State University, Tbilisi, Georgia
16: Also at CERN; European Organization for Nuclear Research, Geneva, Switzerland
17: Also at RWTH Aachen University; III. Physikalisches Institut A, Aachen, Germany
18: Also at University of Hamburg, Hamburg, Germany
19: Also at Brandenburg University of Technology, Cottbus, Germany
20: Also at MTA-ELTE Lendület CMS Particle and Nuclear Physics Group; Eötvös Loránd University, Budapest, Hungary
21: Also at Institute of Nuclear Research ATOMKI, Debrecen, Hungary
22: Also at Institute of Physics; University of Debrecen, Debrecen, Hungary
23: Also at Indian Institute of Technology Bhubaneswar, Bhubaneswar, India
24: Also at Institute of Physics, Bhubaneswar, India
25: Also at Shoolini University, Solan, India
26: Also at University of Visva-Bharati, Santiniketan, India
27: Also at University of Ruhuna, Matara, Sri Lanka
28: Also at Isfahan University of Technology, Isfahan, Iran
29: Also at Yazd University, Yazd, Iran
30: Also at Plasma Physics Research Center; Science and Research Branch; Islamic Azad University, Tehran, Iran
31: Also at Università degli Studi di Siena, Siena, Italy
32: Also at INFN Sezione di Milano-Bicocca; Università di Milano-Bicocca, Milano, Italy
33: Also at International Islamic University of Malaysia, Kuala Lumpur, Malaysia
34: Also at Malaysian Nuclear Agency; MOSTI, Kajang, Malaysia
35: Also at Consejo Nacional de Ciencia y Tecnología, Mexico city, Mexico
36: Also at Warsaw University of Technology; Institute of Electronic Systems, Warsaw, Poland
37: Also at Institute for Nuclear Research, Moscow, Russia

38: Now at National Research Nuclear University 'Moscow Engineering Physics Institute' (MEPhI), Moscow, Russia
39: Also at St. Petersburg State Polytechnical University, St. Petersburg, Russia
40: Also at University of Florida, Gainesville, USA
41: Also at P.N. Lebedev Physical Institute, Moscow, Russia
42: Also at California Institute of Technology, Pasadena, USA
43: Also at Budker Institute of Nuclear Physics, Novosibirsk, Russia
44: Also at Faculty of Physics; University of Belgrade, Belgrade, Serbia
45: Also at INFN Sezione di Pavia; Università di Pavia, Pavia, Italy
46: Also at University of Belgrade; Faculty of Physics and Vinca Institute of Nuclear Sciences, Belgrade, Serbia
47: Also at Scuola Normale e Sezione dell'INFN, Pisa, Italy
48: Also at National and Kapodistrian University of Athens, Athens, Greece
49: Also at Riga Technical University, Riga, Latvia
50: Also at Universität Zürich, Zurich, Switzerland
51: Also at Stefan Meyer Institute for Subatomic Physics (SMI), Vienna, Austria
52: Also at Adiyaman University, Adiyaman, Turkey
53: Also at Istanbul Aydin University, Istanbul, Turkey
54: Also at Mersin University, Mersin, Turkey
55: Also at Piri Reis University, Istanbul, Turkey
56: Also at Izmir Institute of Technology, Izmir, Turkey
57: Also at Necmettin Erbakan University, Konya, Turkey
58: Also at Marmara University, Istanbul, Turkey
59: Also at Kafkas University, Kars, Turkey
60: Also at Istanbul Bilgi University, Istanbul, Turkey
61: Also at Rutherford Appleton Laboratory, Didcot, United Kingdom
62: Also at School of Physics and Astronomy; University of Southampton, Southampton, United Kingdom
63: Also at Monash University; Faculty of Science, Clayton, Australia
64: Also at Instituto de Astrofísica de Canarias, La Laguna, Spain
65: Also at Bethel University, ST. PAUL, USA
66: Also at Utah Valley University, Orem, USA
67: Also at Purdue University, West Lafayette, USA
68: Also at Beykent University, Istanbul, Turkey
69: Also at Bingol University, Bingol, Turkey
70: Also at Erzincan University, Erzincan, Turkey
71: Also at Sinop University, Sinop, Turkey
72: Also at Mimar Sinan University; Istanbul, Istanbul, Turkey
73: Also at Texas A&M University at Qatar, Doha, Qatar
74: Also at Kyungpook National University, Daegu, Korea